2007-12

Ignition characteristics for transient plasma ignition of ethylene/air and JP-10/air mixtures in a Pulse Detonation Engine

Hackard, Charles N.

Monterey California. Naval Postgraduate School

NAVAL POSTGRADUATE SCHOOL

MONTEREY, CALIFORNIA

THESIS

IGNITION CHARACTERISTICS FOR TRANSIENT PLASMA IGNITION OF ETHYLENE/AIR AND JP-10/AIR MIXTURES IN A PULSE DETONATION ENGINE

by

Charles N. Hackard, Jr.

December 2007

Thesis Advisor: Christopher M. Brophy
Second Reader: Jose Sinibaldi

Approved for public release; distribution is unlimited

THIS PAGE INTENTIONALLY LEFT BLANK

REPORT DOCUMENTATION PAGE			Form Approved OMB No. 0704-0188
Public reporting burden for this collection of information is estimated to average 1 hour per response, including the time for reviewing instruction, searching existing data sources, gathering and maintaining the data needed, and completing and reviewing the collection of information. Send comments regarding this burden estimate or any other aspect of this collection of information, including suggestions for reducing this burden, to Washington headquarters Services, Directorate for Information Operations and Reports, 1215 Jefferson Davis Highway, Suite 1204, Arlington, VA 22202-4302, and to the Office of Management and Budget, Paperwork Reduction Project (0704-0188) Washington DC 20503.			
1. AGENCY USE ONLY *(Leave blank)*	**2. REPORT DATE** December 2007	**3. REPORT TYPE AND DATES COVERED** Master's Thesis	
4. TITLE AND SUBTITLE Ignition Characteristics for Transient Plasma Ignition of Ethylene/air and JP-10/Air Mixtures in a Pulse Detonation Engine		**5. FUNDING NUMBERS**	
6. AUTHOR(S) Charles N. Hackard, Jr.			
7. PERFORMING ORGANIZATION NAME(S) AND ADDRESS(ES) Naval Postgraduate School Monterey, CA 93943-5000		**8. PERFORMING ORGANIZATION REPORT NUMBER**	
9. SPONSORING /MONITORING AGENCY NAME(S) AND ADDRESS(ES) N/A		**10. SPONSORING/MONITORING AGENCY REPORT NUMBER**	
11. SUPPLEMENTARY NOTES The views expressed in this thesis are those of the author and do not reflect the official policy or position of the Department of Defense or the U.S. Government.			
12a. DISTRIBUTION / AVAILABILITY STATEMENT Approved for public release; distribution is unlimited		**12b. DISTRIBUTION CODE**	

13. ABSTRACT (maximum 200 words)

The inlet mass flow, fuel injection profile, igniter characteristics, ignition delay, and operational frequency all dictate the success of a Pulse Detonation Engine (PDE). An optical sensor was developed and utilized for the observation of ignition zone characteristics over varying refresh conditions that showed decreasing ignition delay times when approaching marginally fuel-rich reactant mixtures. A wide range of equivalence ratios for ethylene/air mixtures were explored and a limited number of JP-10/air mixtures. The JP-10/air fuel mixtures were nearly impossible to ignite at characteristic velocities greater than 35 m/s until a porous ignition shield was installed. The porous shield, surrounding the Transient Plasma Ignition (TPI) electrode, demonstrated the successful ignition at characteristic velocities up to 100 m/s for C_2H_4/air and 55 m/s for JP-10/air mixtures. The ignition shield slowed down a portion of the fuel-air mixture to increase the local residence time, allowing for more reliable ignition. The resulting combustion products proceeded to ignite the remaining fuel-air mixture. The ignition shield design appears to locally prevent a complete purge of the previous cycle's products, and a transient plasma discharge was still required for subsequent ignition to occur. This effect further reduced the observed ignition delay time in ethylene/air and JP-10/air fuel mixtures.

14. SUBJECT TERMS - Pulse Detonation Engine, PDE, Transient Plasma Ignition, TPI, Detonation, Deflagration, JP-10			**15. NUMBER OF PAGES** 63
			16. PRICE CODE
17. SECURITY CLASSIFICATION OF REPORT Unclassified	**18. SECURITY CLASSIFICATION OF THIS PAGE** Unclassified	**19. SECURITY CLASSIFICATION OF ABSTRACT** Unclassified	**20. LIMITATION OF ABSTRACT** UU

NSN 7540-01-280-5500 Standard Form 298 (Rev. 2-89)
Prescribed by ANSI Std. 239-18

THIS PAGE INTENTIONALLY LEFT BLANK

Approved for public release; distribution is unlimited

IGNITION CHARACTERISTICS FOR TRANSIENT PLASMA IGNITION OF ETHYLENE/AIR AND JP-10/AIR MIXTURES IN A PULSE DETONATION ENGINE

Charles N. Hackard, Jr.
Lieutenant Commander, United States Navy
B.S. in Mechanical Engineering, University of Arizona, 1995

Submitted in partial fulfillment of the
requirements for the degree of

MASTER OF SCIENCE IN ASTRONAUTICAL ENGINEERING

from the

NAVAL POSTGRADUATE SCHOOL
December 2007

Author: Charles N. Hackard, Jr.

Approved by: Christopher M. Brophy
Thesis Advisor

Jose O. Sinibaldi
Second Reader

Anthony J. Healey
Chairman, Department of Mechanical & Astronautical Engineering

THIS PAGE INTENTIONALLY LEFT BLANK

ABSTRACT

The inlet mass flow, fuel injection profile, igniter characteristics, ignition delay, and operational frequency all dictate the success of a Pulse Detonation Engine (PDE). An optical sensor was developed and utilized for the observation of ignition zone characteristics over varying refresh conditions that showed decreasing ignition delay times when approaching marginally fuel-rich reactant mixtures. A wide range of equivalence ratios for ethylene/air mixtures were explored and a limited number of JP-10/air mixtures. The JP-10/air fuel mixtures were nearly impossible to ignite at characteristic velocities greater than 35 m/s until a porous ignition shield was installed. The porous shield, surrounding the Transient Plasma Ignition (TPI) electrode, demonstrated the successful ignition at characteristic velocities up to 100 m/s for C_2H_4/air and 55 m/s for JP-10/air mixtures. The ignition shield slowed down a portion of the fuel-air mixture to increase the local residence time, allowing for more reliable ignition. The resulting combustion products proceeded to ignite the remaining fuel-air mixture. The ignition shield design appears to locally prevent a complete purge of the previous cycle's products, and a transient plasma discharge was still required for subsequent ignition to occur. This effect further reduced the observed ignition delay time in ethylene/air and JP-10/air fuel mixtures.

THIS PAGE INTENTIONALLY LEFT BLANK

TABLE OF CONTENTS

I. INTRODUCTION....1
A. HIGH SPEED PROPULSION TRADE SPACE....1
B. TRANSIENT PLASMA IGNITION....4
C. OBJECTIVES OF THE THESIS RESEARCH....5

II. BACKGROUND....7
A. INTRODUCTION....7
B. DETONATION THERMODYNAMICS....7
C. DE CYCLE....9

III. DESIGN....13
A. ELECTRODE....13
B. MACOR® INSULATOR....15
C. POROUS SHIELD COMBUSTION CHAMBER....18

IV. EXPERIMENTAL SETUP....21
A. NPS PULSE DETONATION ENGINE....21
B. OPTICAL SENSOR....22
C. VITIATOR....24
D. FACILITY AND PDE CONTROL....25
E. DATA ACQUISITION....26

V. RESULTS....29
A. ETHYLENE/AIR....29
B. JP-10/AIR....33
C. ETHYLENE/AIR WITH POROUS IGNITION SHIELD....35
D. JP-10/AIR WITH POROUS IGNITION SHIELD....36

VI. CONCLUSIONS AND FUTURE WORK....39
A. CONCLUSIONS....39
B. FUTURE WORK....39

APPENDIX A: NPS ROCKET LAB TEST CELL #2 SOP....41

LIST OF REFERENCES....45

INITIAL DISTRIBUTION LIST....47

THIS PAGE INTENTIONALLY LEFT BLANK

LIST OF FIGURES

Figure 1. Performance Comparison of High-Speed Propulsion Technologies 2
Figure 2. Specific thrust, $F/\dot{m}_o$, of ideal PDE and Brayton cycles as functions of ψ.....3
Figure 3. Specific fuel consumption S, of ideal PDE and Brayton cycles as functions of ψ.....3
Figure 4. Streamer Field from TPI electrode [6].....4
Figure 5. Schematic Diagram of a Stationary 1-D Combustion Wave (Deflagration or Detonation) 8
Figure 6. 2-D Detonation front structure consisting of multiple shock waves and reaction zones.....9
Figure 7. Valveless PDE Operating Cycle 10
Figure 8. Stainless Steel Electrode Solid Model 13
Figure 9. Actual Stainless Steel Electrode 13
Figure 10. Stainless Steel Electrode 14
Figure 11. Side View of Macor and Electrode inside the PDE 15
Figure 12. Previous Macor Insulator Design Failures.....16
Figure 13. New Macor Insulator Design 16
Figure 14. Macor Insulator Sleeve Solid Model 17
Figure 15. Macor Insulator Sleeve 17
Figure 16. Porous Ignition Shield.....18
Figure 17. Stainless Steel Tube of the Porous Ignition Shield 19
Figure 18. Stainless Steel Core of the Porous Ignition Shield 19
Figure 19. Porous Ignition Shield installed in the ignition zone of the PDE 20
Figure 20. NPS Pulse Detonation Engine 21
Figure 21. Optical Sensor in Initiation Section 22
Figure 22. Optical Setup Diagram.....23
Figure 23. Ignition Command, Optical, and Pressure Transducer Characterization.....24
Figure 24. Hydrogen/Air Vitiator.....25
Figure 25. Propulsion Lab Test Cell #2 Graphics-User Interface 26
Figure 26. Optical, TPI, and Pressure Transducer Data Collection Interface 27
Figure 27. 90% Equivalence Ratio for $\dot{m}_{air}$ = 0.35 kg/s for Single Orifice.....30
Figure 28. Ignition Delay vs. Fuel Pressure for C_2H_4/air for $\dot{m}_{air}$ = 0.3125 kg/s 31
Figure 29. Ignition Delay vs. Equivalence Raito for C_2H_4/air for $\dot{m}_{air}$ = 0.3125 kg/s.....31
Figure 30. Ignition Delay vs. Fuel Pressure for C_2H_4/air for $\dot{m}_{air}$ = 0.35 kg/s 32
Figure 31. Ignition Delay vs. Equivalence Ratio for C_2H_4/air for $\dot{m}_{air}$ = 0.35 kg/s.....32
Figure 32. Ignition Delay vs. Fuel Pressure for C_2H_4/air for $\dot{m}_{air}$ = 0.4 kg/s 33
Figure 33. JP10 Fuel Profiles for Two Injectors [12].....34
Figure 34. Incomplete Purge for $\dot{m}_{air}$ = 0.45 kg/s with Ignition Shield.....36
Figure 35. Successful JP-10/air Ignition for $\dot{m}_{air}$ = 0.15 kg/s.....37
Figure 36. Successful JP-10/air Ignition for $\dot{m}_{air}$ = 0.2 kg/s.....37

Figure 37. JP-10/air Ignition after Vitiator Cutoff 38

LIST OF TABLES

Table 1. Qualitative Differences between Detonation and Deflagration 8

THIS PAGE INTENTIONALLY LEFT BLANK

ACKNOWLEDGMENTS

The author would like to express his profound gratitude to Professor Christopher Brophy for the help, guidance, and education he provided while pursuing this thesis work. His clear dedication to research and education was admired and appreciated.

The author would also like to thank Mr. George Hageman for his extensive work, technical expertise, and enthusiasm at the Rocket Propulsion and Combustion Laboratory at the Naval Postgraduate School.

Finally, the author would like to express his deep gratitude for the support of his wife, Meghan, in this and all endeavors.

THIS PAGE INTENTIONALLY LEFT BLANK

I. INTRODUCTION

Practical Pulse Detonation Engines (PDE) will be based on storable liquid hydrocarbon fuels such as JP-10. Gaseous fuels possess low energy densities, and are impractical for tactical weapons that often have significant volume constraints. A liquid-fueled engine will be required for practical application because of the higher specific energy density and the reduced volume/storage requirements, but the injection/atomization process and associated slow chemical kinetics remain challenging barriers.

A large component to the future of a time-critical strike capability lies with a high supersonic strike weapon. The supersonic speed will greatly decrease the time to target and may contribute to the effectiveness of a kinetic penetrator against buried targets. Increased thermodynamic efficiency, lower operational cost, and the simple design inherent in PDE systems should allow them to be readily adopted for use in tactical propulsion applications.

A. HIGH SPEED PROPULSION TRADE SPACE

A PDE is a possible propulsion system for an expendable tactical platform, and the inherent repetitive detonation process places it in the unsteady, frequency intermittent class of air-breathing engines. Depending on the mission specifics, a PDE may have practical advantages over the turbojet, ramjet, or solid motors, which are all steady-state devices. A common figure of merit for air-breathing engines is the fuel-based specific impulse, displayed in equation 1.

$$Isp_f = \frac{F_{net}}{\dot{m}_f g_o} \qquad [1]$$

where F_{net} = net thrust

$\dot{m}_f$ = fuel mass flow rate

g_o = gravitational constant

Figure 1 depicts the specific impulse of various propulsion systems over their practical flight Mach number ranges [1, 2].

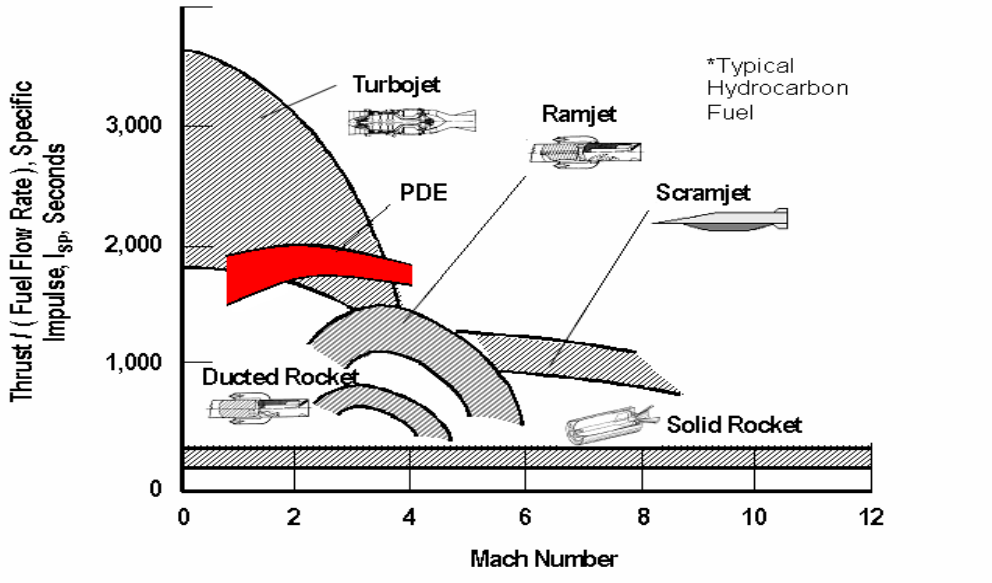

Figure 1. Performance Comparison of High-Speed Propulsion Technologies

Turbojets are better suited for subsonic applications due to the benefits of the mechanical compression where as above flight Mach numbers of around 2.0, the inlet compression delivers sufficient inlet conditions to the combustor. Extensive cooling is also needed for the turbine inlet to avoid exceeding material temperature limits. Since PDEs require no compressors or turbines, they are generally simpler in design and potentially have a higher thrust-to-weight ratio.

The PDE has also been predicted to outperform the ramjet for its given Mach number ranges. A rocket boost is required to get a ramjet up to its initial operating speed, while the PDE can operate from subsonic to supersonic speeds as long as the inlet is properly designed. A ramjet decelerates the inlet airflow for subsonic combustion before accelerating the products through a nozzle. Most PDE systems initially ignite a subsonic combustion wave and then accelerate the flame to a detonation by way of a deflagration to detonation transition (DDT) process, which results in the formation of a detonation and a near constant volume combustion event [4]. Figures 2 and 3 details the advantages of the ideal Humphrey-like PDE cycle over the Brayton ramjet cycles for specific thrust and specific fuel consumption [3]. The symbol ψ is the cycle thermal compression ratio, and $\tilde{q}$ is the dimensionless heat release. At lower Mach numbers, the ideal PDE produces a higher specific thrust while also consuming less specific fuel that the ramjet.

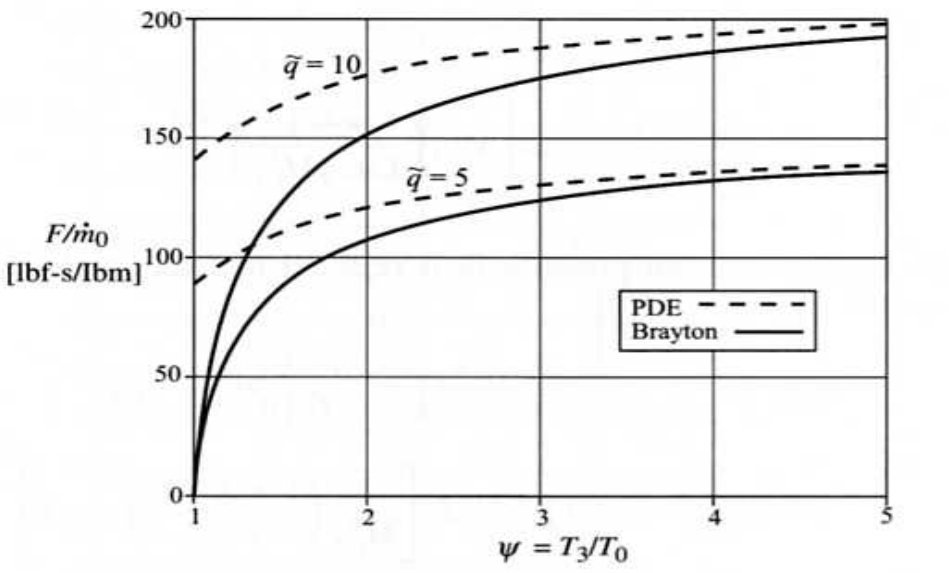

Figure 2. Specific thrust, $F/\dot{m}_o$, of ideal PDE and Brayton cycles as functions of ψ.

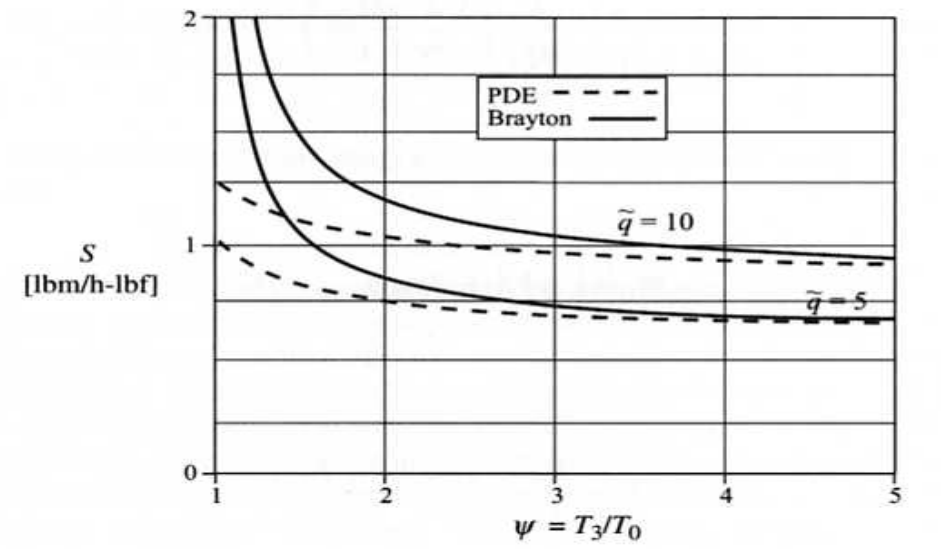

Figure 3. Specific fuel consumption S, of ideal PDE and Brayton cycles as functions of ψ.

Although PDE systems have the ability to takeoff without auxiliary propulsion, most tactical applications will involve some form of booster. While acoustics, vibration, and material properties will probably prevent a pure PDE-based system from being used for a manned propulsion system, the tactical realm remains the most likely application for

this technology. As research and development efforts continue with the University of Southern California's Transient Plasma Ignition system and alternative detonation formation techniques, the observed performance is moving towards theoretical values.

B. TRANSIENT PLASMA IGNITION

The NPS Rocket Propulsion Lab and University of Southern California are jointly investigating the application of a Transient Plasma Ignition (TPI) to PDE ignition. The TPI utilizes a pseudo spark or corona discharge that occurs in tens of nanoseconds [4, 5]. A corona discharge is the segment of an electric discharge before the onset of a low-voltage, high current arc that essentially creates plasma in the transient or formative stage [5]. The TPI system delivers pulses of 70 to 100 kV within 50 to 100 ns at currents from 450 to 600 A, and creates electrons with energy levels of 10-30 eV [2]. The TPI uses a threaded electrode to distribute the ignition energy through hundreds of streamers. The streamers generate reactive species such as O atoms, H atoms, OH, and CH radicals, which quickly react to produce chain branching reactions [6]. Figure 4 depicts the corona discharge.

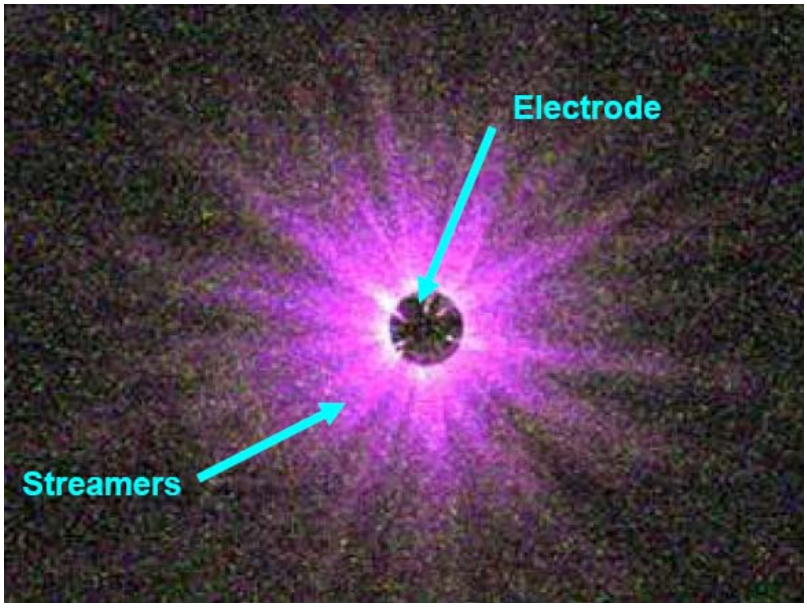

Figure 4. Streamer Field from TPI electrode [6]

C. OBJECTIVES OF THE THESIS RESEARCH

The primary objectives were to verify that a TPI discharge into the initiation chamber occurred for each cycle and then measure the resulting ignition delay times for ethylene/air and JP-10/air mixtures. A range of air flow mass and equivalence ratios was explored and ignition delay times were determined based on output from the optical sensor. The optical system complements the pressure transducers data in order to distinctly characterize the ignition and DDT processes, and provides a relationship between refresh velocities, fuel/air ratios, TPI characteristics, and ignition timing. The ultimate goal was to achieve successful ignition and initiation of high velocity ethylene/air flow fields, and then apply that knowledge base to obtain successful JP-10/air detonations.

THIS PAGE INTENTIONALLY LEFT BLANK

II. BACKGROUND

A. INTRODUCTION

The use of intermittent pulse detonation can be traced back to Germany's Hoffman in the late 1930s [7]. The Chapman-Jouguet theory that is represented on the classic Hugoniot curve for combustion and detonation was independently determined by Chapman (1899) and Jouguet (1901-1905). The theory states that the combustion products from a detonation wave propagate away from the wave at sonic speeds relative to the detonation wave. The promising potential of pulse detonation technology has attracted the attention of major engine manufactures like Pratt & Whitney and General Electric. As both companies continue to squeeze diminishing returns on performance out of gas turbine technology, proponents view PDEs as possibly providing a quantum leap in technology for the next generation of military and commercial propulsion [13]. The fast energy conversion rates of a detonation, as well as a higher theoretical thermodynamic efficiency than a deflagration (constant pressure) process, are the thermodynamic arguments for this system and the motivation for additional research [4].

B. DETONATION THERMODYNAMICS

Pulse Detonation Engines require the detonation of fuel and air to provide the thermodynamic advantage over the ramjet's deflagration combustion process. Deflagration is a nearly constant-pressure process that produces a relatively slow, subsonic combustion wave with a small pressure rise. In deflagration, the combustion wave propagates at a subsonic velocity, roughly 1 to 10 meters per second, is sustained in an almost constant pressure condition. The transport of thermal energy and reactants govern the flame front propagation rate.

Detonation is a nearly constant-volume, supersonic combustion event in which a combustion wave is coupled to a supersonic shock wave. The strong leading shock is sustained by the rapid energy release occurring in a high temperature, highly compressed region immediately behind the leading shock. This close union of the rapid combustion

region and strong shock wave is known as a detonation wave. A detonation wave often propagates at velocities near 2,000 meters per second for most hydrocarbon/air mixtures.

The classical detonation wave structure is described as a one-dimensional leading shock wave followed by the reaction zone propagating at a steady velocity. This structure is commonly referred to as the Zeldovich von Neumann Doring (ZND) structure. A one dimensional (1-D) stationary combustion wave is modeled in Figure 5 [8]. The large thermodynamic property differences of detonation versus deflagration are shown in Table 1 [9].

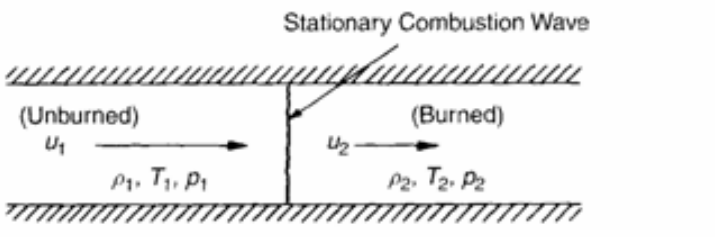

Figure 5. Schematic Diagram of a Stationary 1-D Combustion Wave (Deflagration or Detonation)

	Detonation	**Deflagration**
u_1/c_1	5-10	0.0001-0.03
u_2/u_1	0.4-0.7 (deceleration)	4-16
p_2/p_1	13-55 (compression)	0.98-0.976 (slight expansion)
T_2/T_1	8-21 (heat addition)	4-16 (heat addition)
ρ_2/ρ_1	1.4-2.6	0.06-0.25

Table 1. Qualitative Differences between Detonation and Deflagration

The ZND structure is unstable due to the nonlinear coupling of gasdynamics and energy release which is a further result of the strong sensitivity of the temperature reaction rate [10]. The shock wave and the reaction zone are coupled and propagate at the Chapman-Jouguet (CJ) detonation velocity. The CJ velocity depends on the mixture's initial pressure, temperature, and energy content. In reality, the detonation wave is a multifaceted 3-D structure comprised of a normal and multiple lateral shock waves and reaction zones. Figure 6 shows the nonplanar leading shockwaves and transverse

propagating shock waves that intersect to form triple points [11]. The reaction zones are closely coupled to the shockwaves with a separation distance, or induction length, based on the reactivity of the mixture.

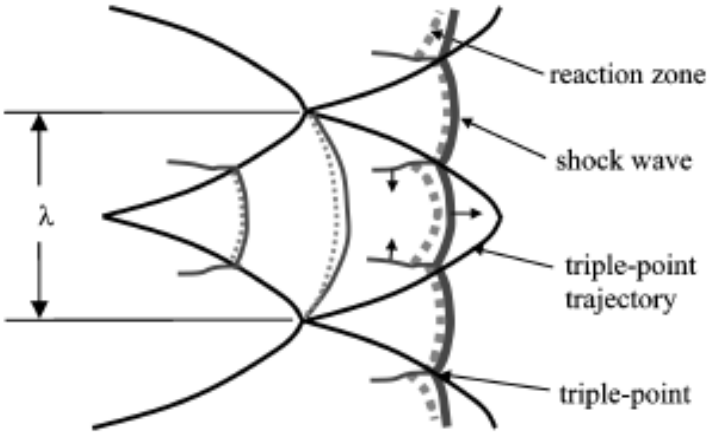

Figure 6. 2-D Detonation front structure consisting of multiple shock waves and reaction zones

C. DE CYCLE

The thermodynamically efficient PDE cycle employs nearly constant volume combustion rather than constant pressure combustion like turbojets and needs to occur many times per second. The system architecture may of may not include the use of a valve to control the air delivery to the combustor. The cycle begins with an injection of fuel upstream of the combustor that produces a fuel/air mixture. The initiator and combustion tube fill with this mixture (1). The ignition event occurs and creates the initial deflagration combustion wave (2). The combustion wave is accelerated and transitions to a detonation wave due to some form of turbulence generating device (3). The detonation wave travels through the remaining unburned fuel and exits the tube (4). A rarefaction wave forms and travels back down the combustion tube and reduces the elevated pressures in the tube (5). The rarefaction wave and the subsequent positive air flow flush out the remaining combustion products in preparation for the next cycle (6). The PDE is then ready for the next cycle (7). Figure 7 depicts the PDE cycle.

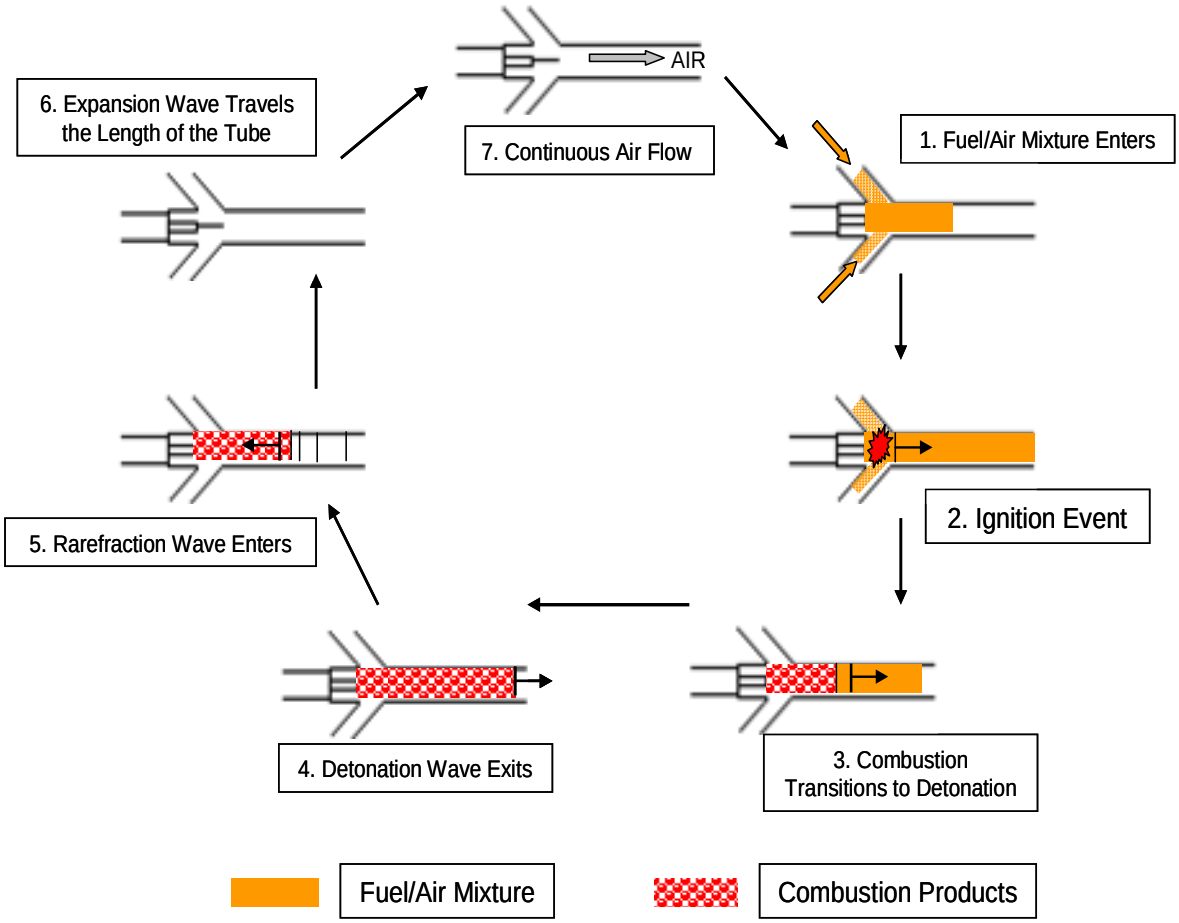

Figure 7. Valveless PDE Operating Cycle

A PDE must operate at a relatively high frequency to produce practical and quasi-steady thrust. For example, a 50 Hz cycle would take up to 20 milliseconds to complete. The combustion tube must fill with fuel, combust and transition to detonation, and finally purge itself in preparation for the next cycle within this time period. Cycle frequencies greater than 60 Hz per tube are likely required to produce sufficient thrust.

The fuel injection timing and detonation initiation delay are the limiting factors. The length and diameter of the tube determine the required volume to fill. For a particular mass flow rate of a reactive mixture, the time required to fill the volume is therefore dictated. Properly scheduling fuel injection with the ignition timing is critical to assure initial combustion and avoid overlapping with the previous cycle. Pre-igniting a new fuel/air mixture prior to a purge would disrupt the cycle. A short initiation delay time and

quick DDT would allow for a reduced cycle time and possibly a shorter tube respectively. High frequency operations require both properties to be reduced as much as possible.

THIS PAGE INTENTIONALLY LEFT BLANK

III. DESIGN

A. ELECTRODE

A new stainless steel rod electrode for the ignition system was designed and built to replace a two piece, dual material electrode. The electrode was threaded on the end, outside of a Macor® insulator, to produce a uniformly distributed corona discharge. The threaded portion of the electrode had a diameter of 0.188 inches, a length of 2 inches, and 20 threads per inch. Figure 8 is the solid model of the stainless steel electrode and Figure 9 is the actual electrode. Figure 10 is the engineering drawing.

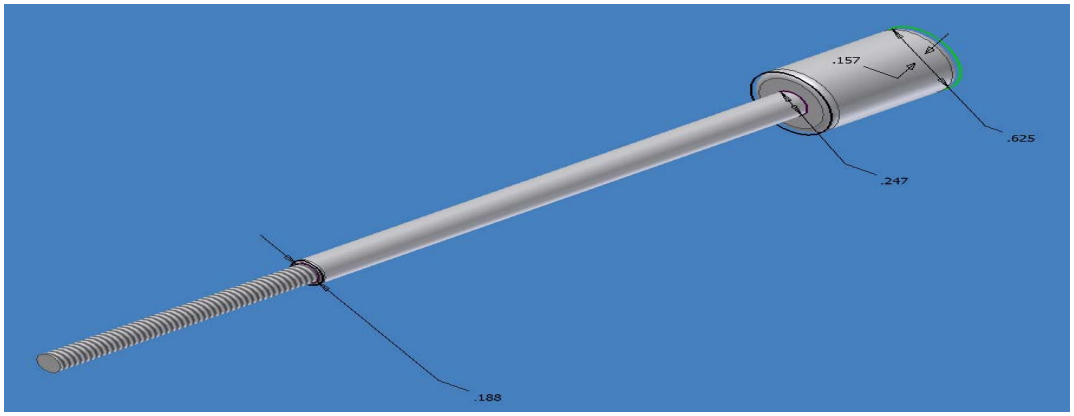

Figure 8. Stainless Steel Electrode Solid Model

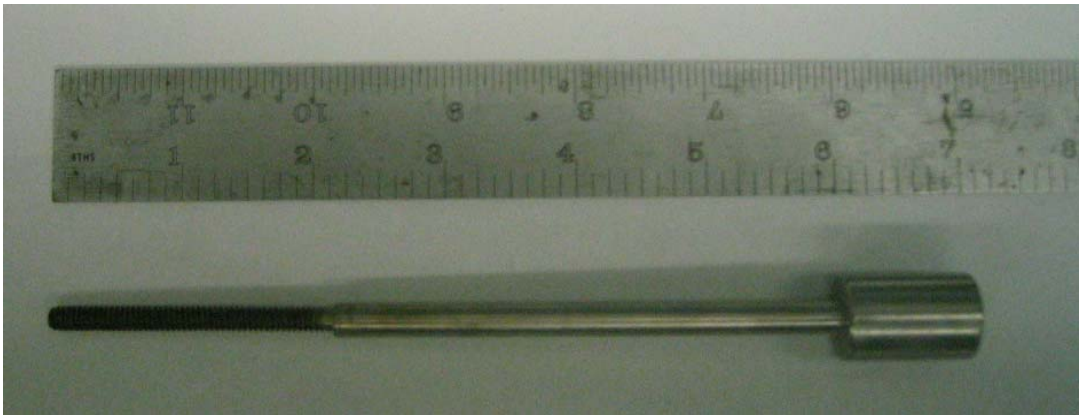

Figure 9. Actual Stainless Steel Electrode

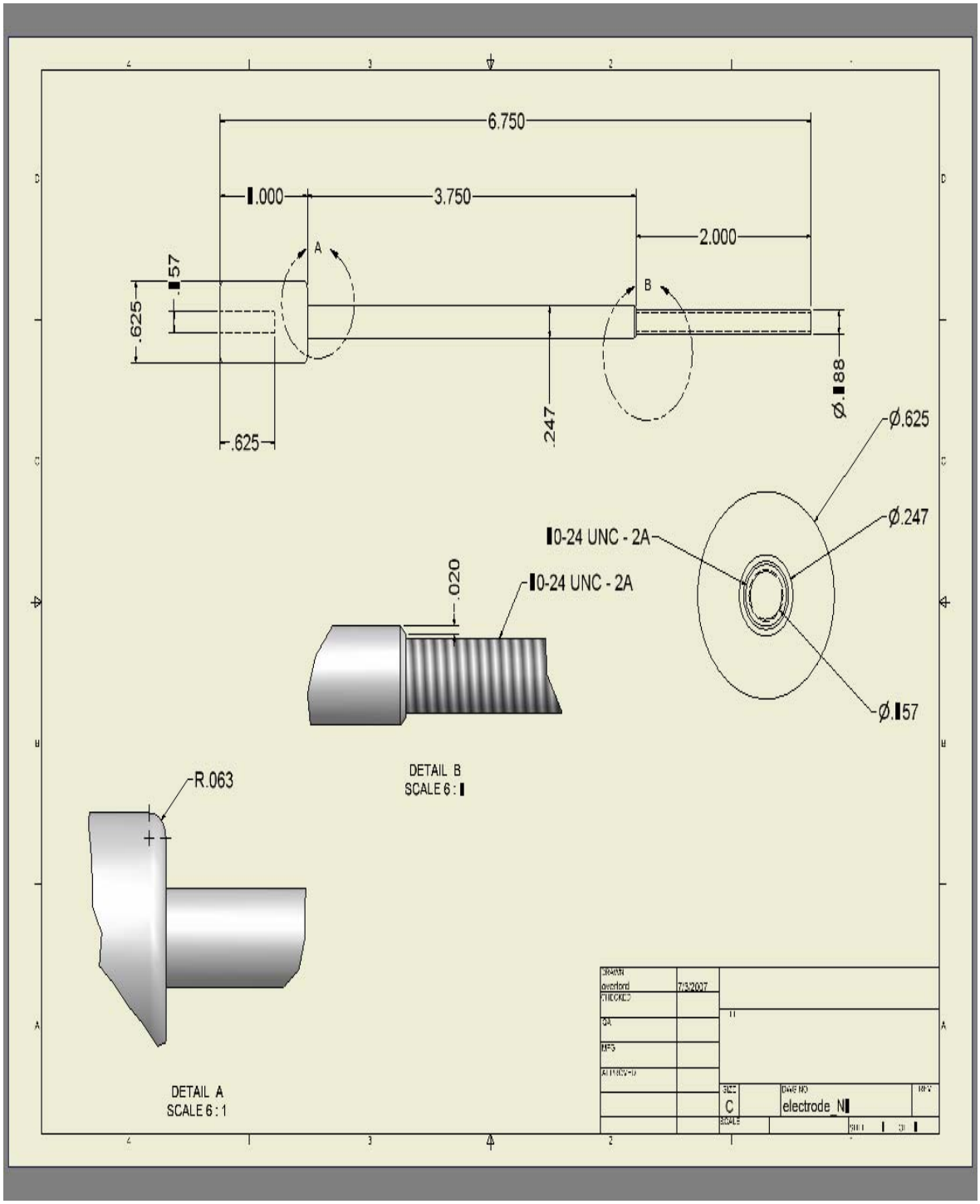

Figure 10. Stainless Steel Electrode

B. MACOR® INSULATOR

Macor is a machineable ceramic with a high dielectric constant, a high temperature capability, and a similar coefficient of thermal expansion to stainless steel. A Macor insulator surrounds and insulates the electrode from the head flange to the middle of the converging arms fuel/air stream.

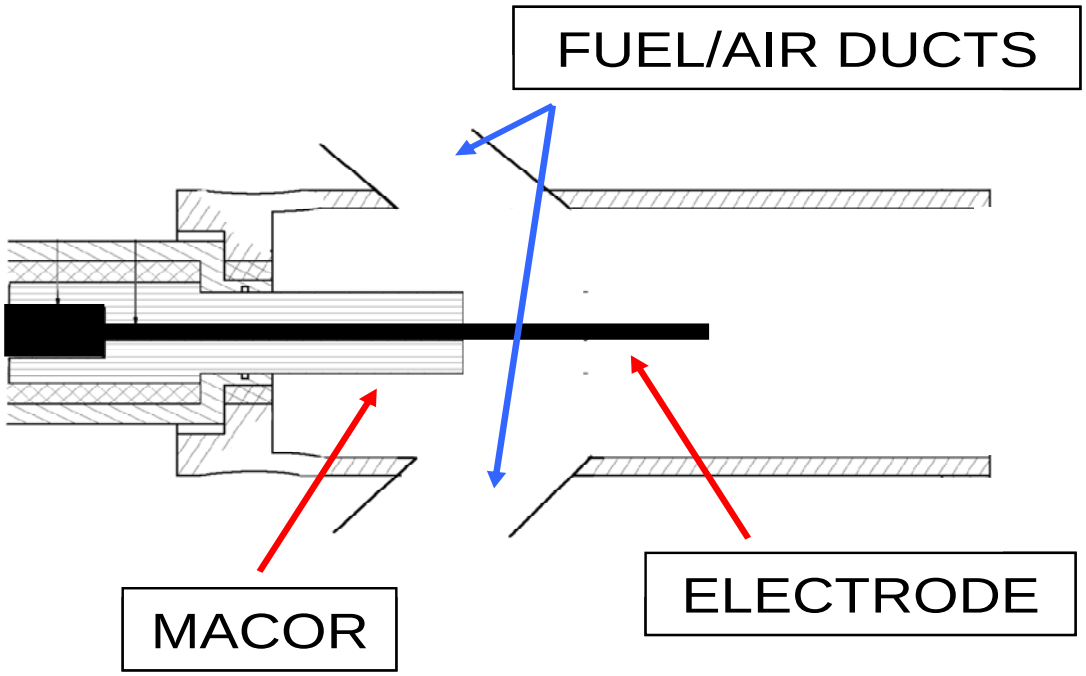

Figure 11. Side View of Macor and Electrode inside the PDE

Previous Macor insulators failed due to mechanical vibration. Typical design life was roughly 4,000 successful combustion producing events which occurred over 1 second intervals. Figure 12 depicts two failures of previous designs involving cracks which started from the insulator/threaded electrode interface.

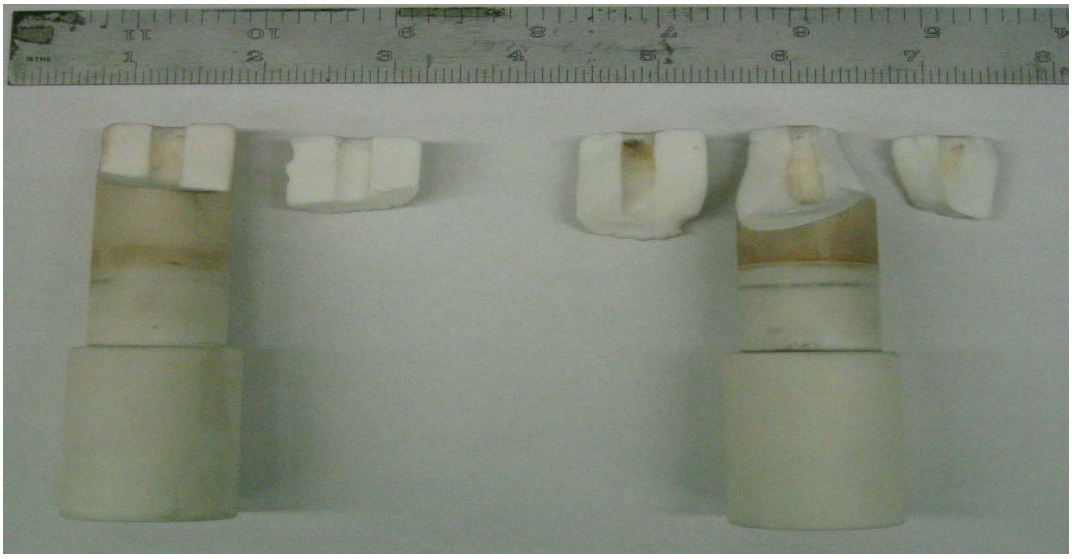

Figure 12. Previous Macor Insulator Design Failures

A new design incorporated an increased diameter opening for the last 0.8 inches of the insulator that extended into the initiation chamber. The wider opening allowed for increased displacement of the electrode before making contact with the Macor. The new design has not failed in over 12,000 cycles of one second, two second, and four second combustion events. Figure 13 is the new Macor design, Figure 14 is the solid model, and Figure 15 is the engineering drawing.

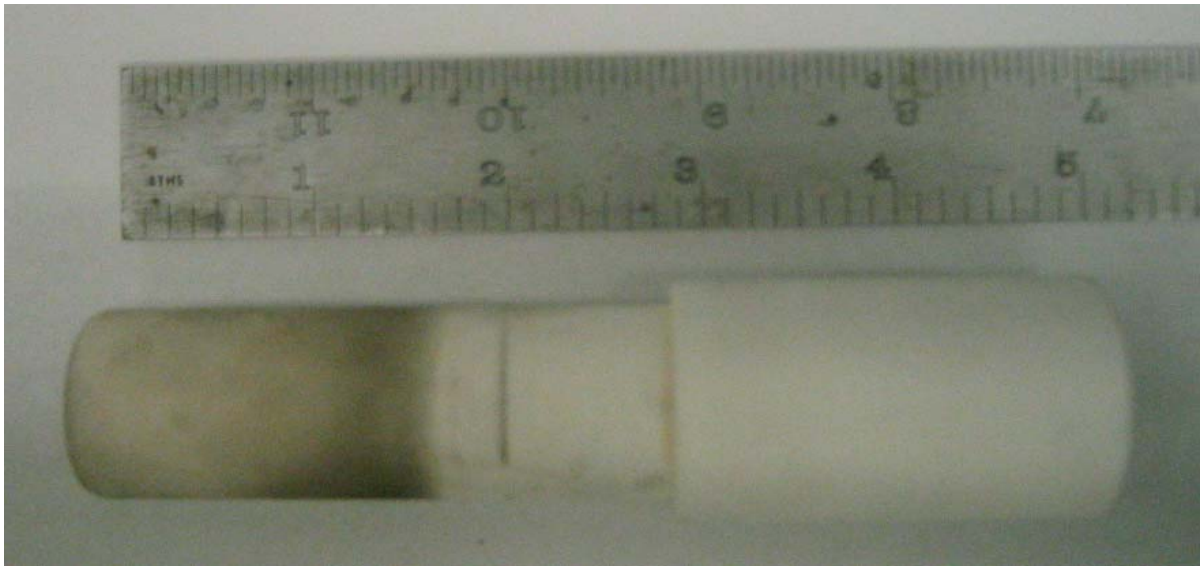

Figure 13. New Macor Insulator Design

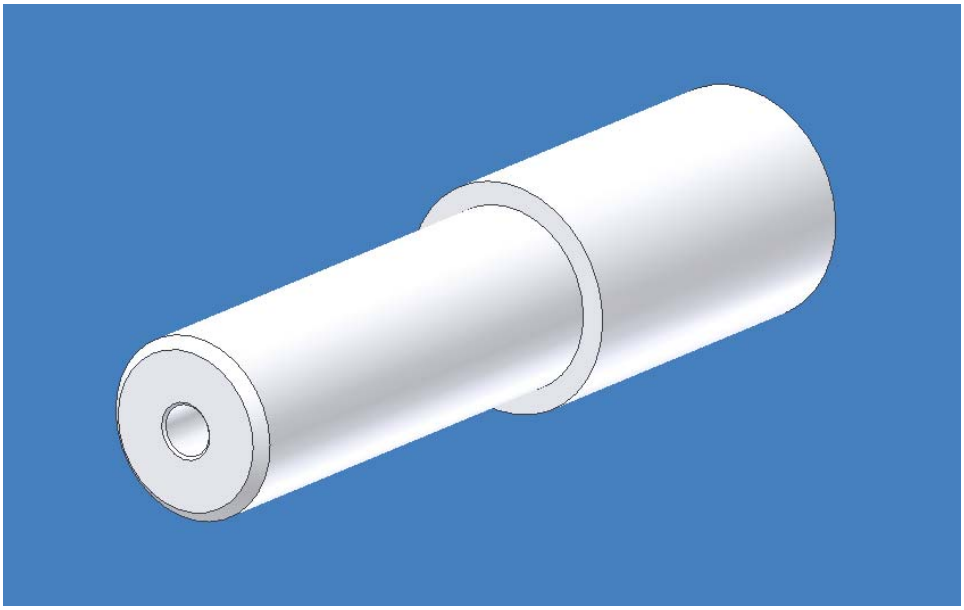

Figure 14. Macor Insulator Sleeve Solid Model

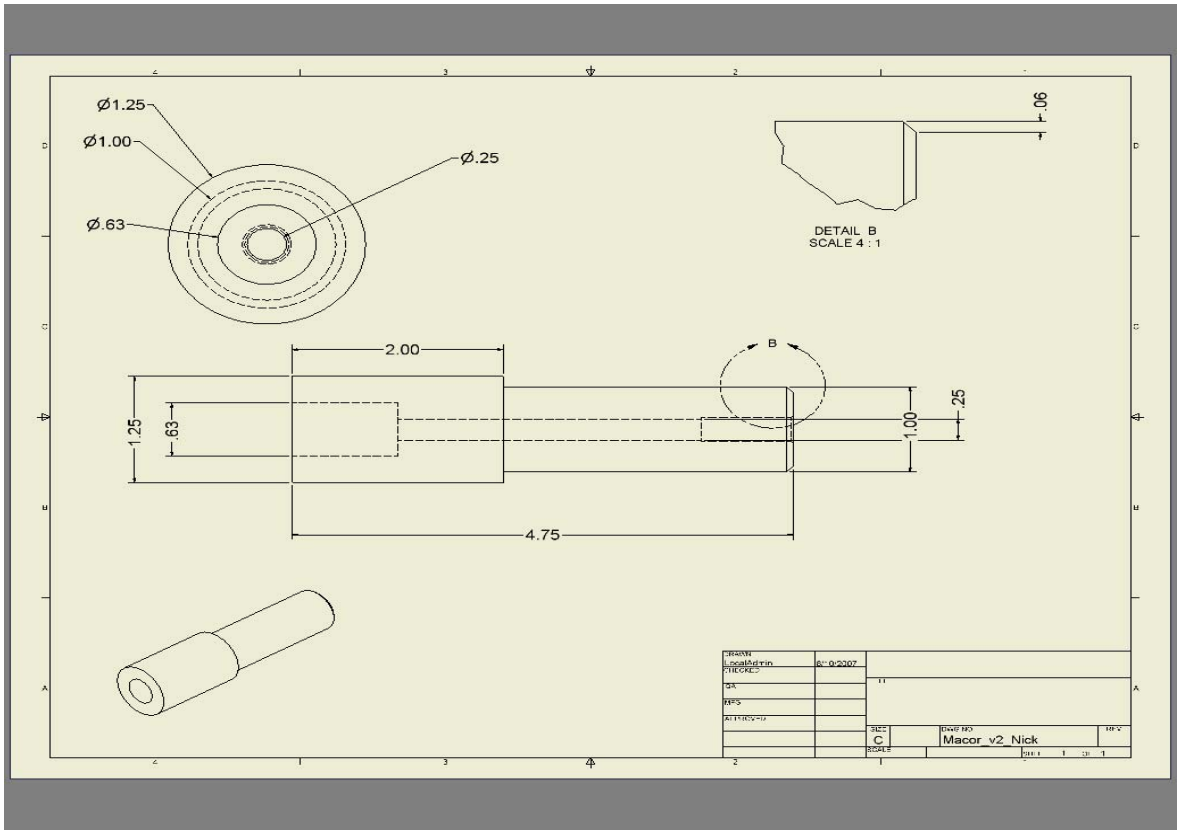

Figure 15. Macor Insulator Sleeve

C. POROUS SHIELD COMBUSTION CHAMBER

A porous ignition shield was required to assist combustion initiation for high velocity ethylene/air and all JP-10/air events. The 25% porous ignition shield provided a lower velocity region for a portion of the fuel/air mixture to enable sufficient ignition and combustion before propagating into the bulk of the rejoining the remaining fuel/air flow.

The stainless steel ignition is comprised of two parts, a metal core to fill an existing recirculation section and a porous metal sleeve to surround the tip of the Macor and the electrode. The two pictures in figure 16 show different views of the ignition shield before it was installed into the PDE. Figures 17 and 18 are the engineering drawings of the metal tube and core separately.

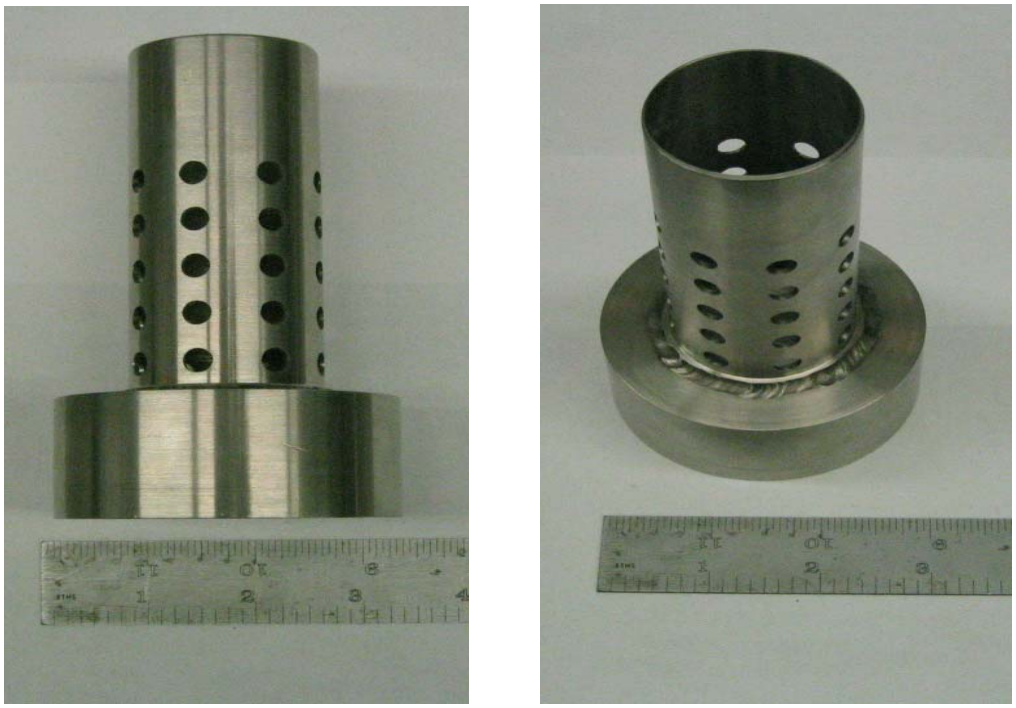

Figure 16. Porous Ignition Shield

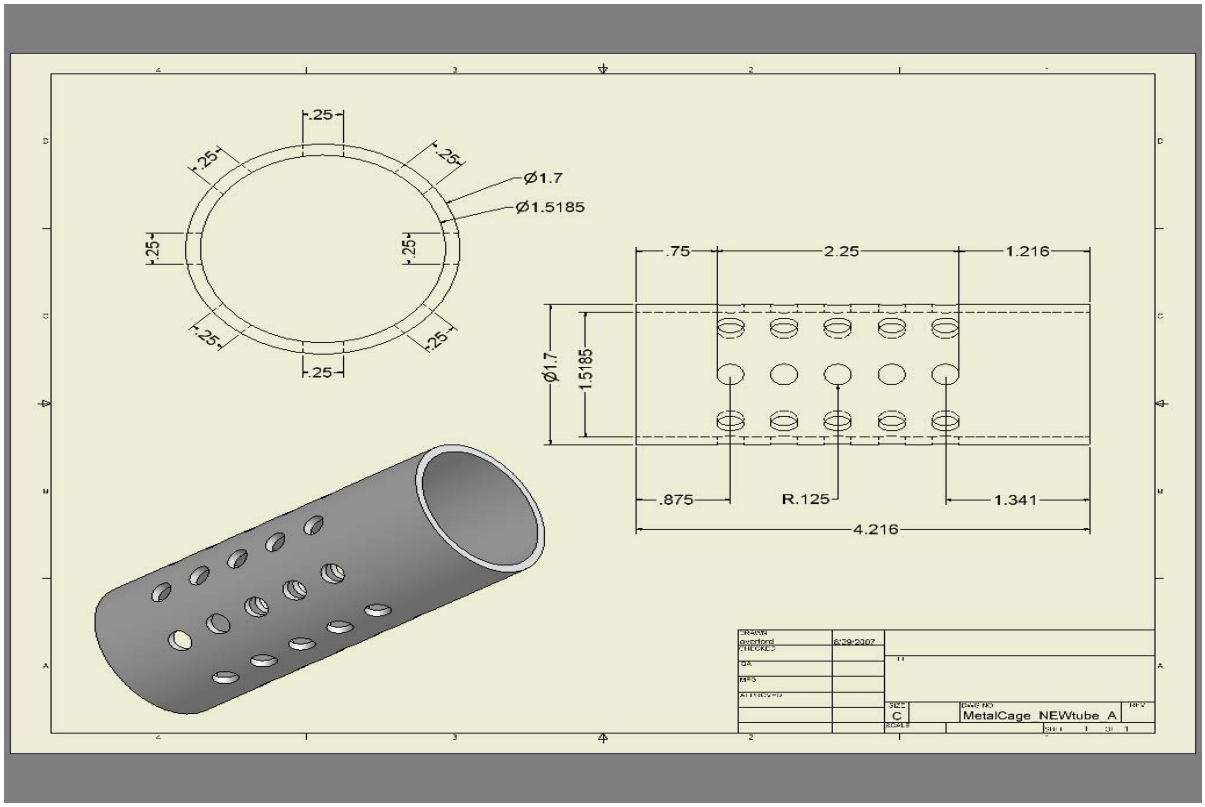

Figure 17. Stainless Steel Tube of the Porous Ignition Shield

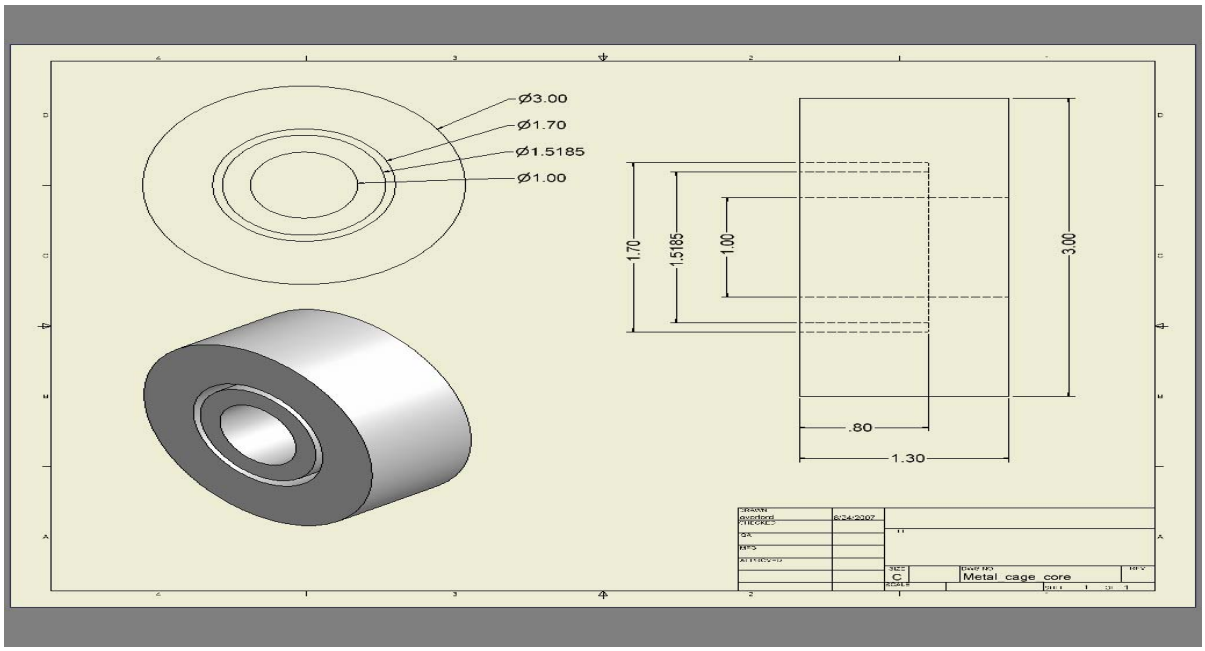

Figure 18. Stainless Steel Core of the Porous Ignition Shield

Figure 19 shows the porous ignition shield installed in the PDE. The TPI electrode and Macor insulator in the ignition zone of the PDE are protected by the shield.

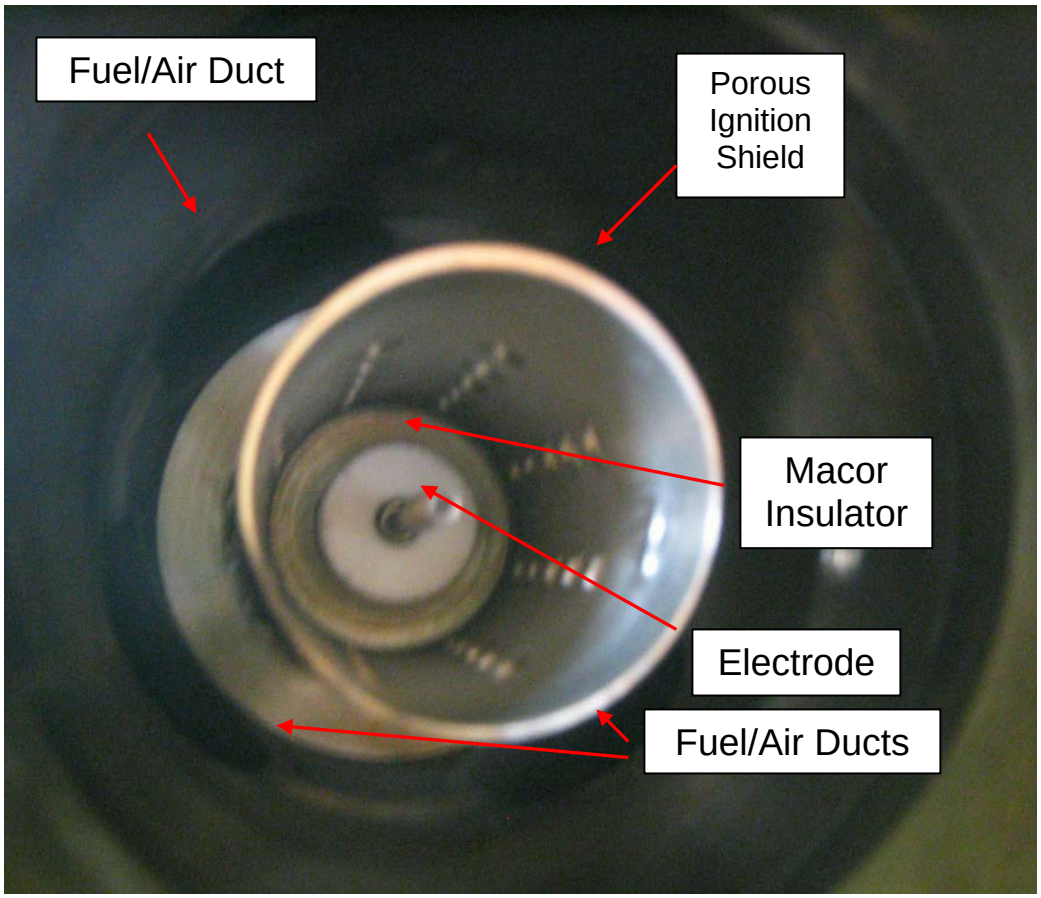

Figure 19. Porous Ignition Shield installed in the ignition zone of the PDE

IV. EXPERIMENTAL SETUP

A. NPS PULSE DETONATION ENGINE

The NPS PDE design utilized a 38 inch (96.5 cm) long and 3 inch (7.62 cm) internal diameter tube with four 45 degree arms which deliver the fuel/air mixture to the combustor. A wall spiral was used to generate turbulence and assist the DDT process. Four JP-10 injectors were installed upstream of a multi-orifice choke in each arm, while four ethylene injectors were positioned downstream of the chokes. Figure 20 depicts the PDE configuration of ethylene and JP-10 injectors, two pressure transducers, an optical sensor, and the four 45 degree inlet arms.

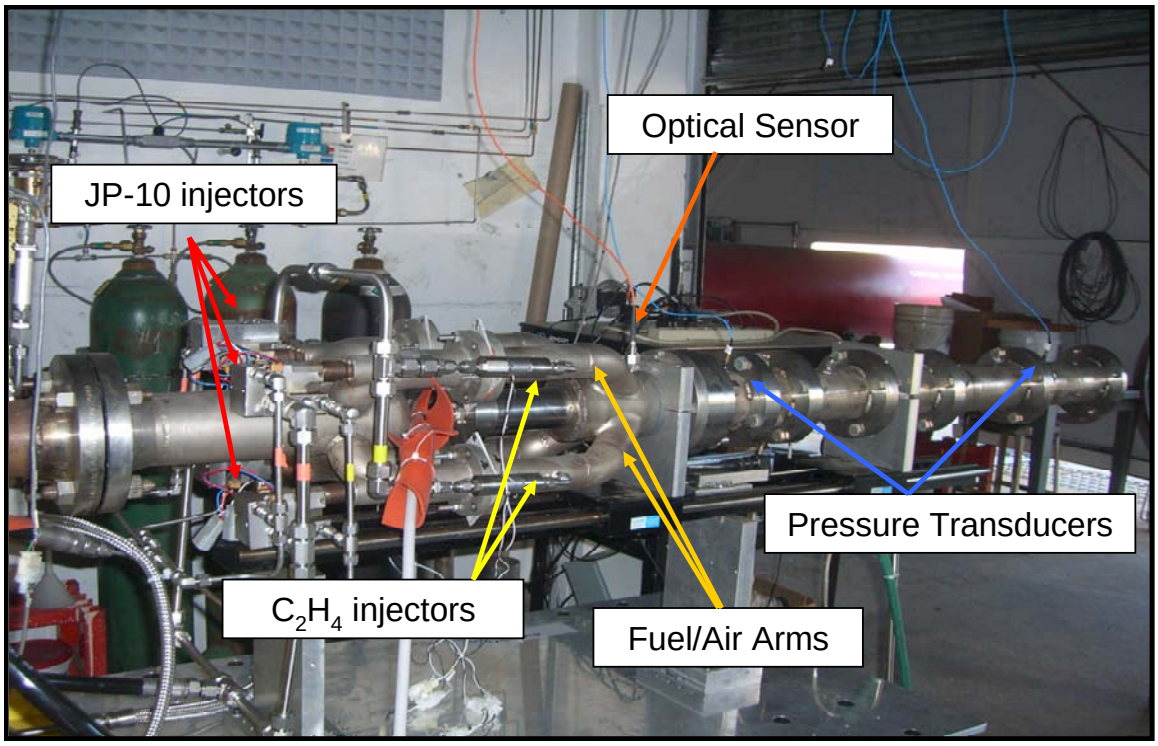

Figure 20. NPS Pulse Detonation Engine

In previous thesis work at NPS, the primary measurement for determining ignition delay time was based on high-frequency pressure measurements. An optical sensor, initially filtered for OH emission, would confirm TPI discharge and initial combustion wave formation. Two high speed Kistler pressure transducers supported the initial optical

readings. The TPI ignition command was also recorded to ensure that the optical sensor was supervising the electrode corona discharge, and that none of the TPI discharges occurred outside of the initiation chamber. Figure 21 shows the optical sensor directly over the tip of the TPI electrode near the head end of the PDE.

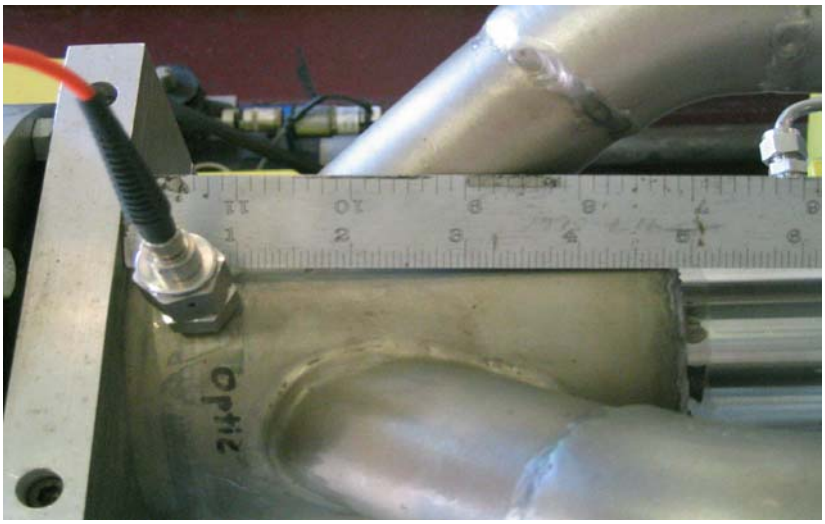

Figure 21. Optical Sensor in Initiation Section

B. OPTICAL SENSOR

The THORLABS PDA10A Wideband Amplified Silicon Detector was used to detect the corona discharge and combustion activity in the ignition area. The PDA10A was a wideband amplified, silicon detector with a detection range from 200-1100 nm. The original application employed a UV filter to detect OH emissions at the 308-310 nm bandwidths during the corona discharge and subsequent combustion. The filter proved to be too restrictive for viewing the entire ignition sequence, so the optical sensor was operated in a broadband mode. Figure 22 is a diagram of the entire optical setup.

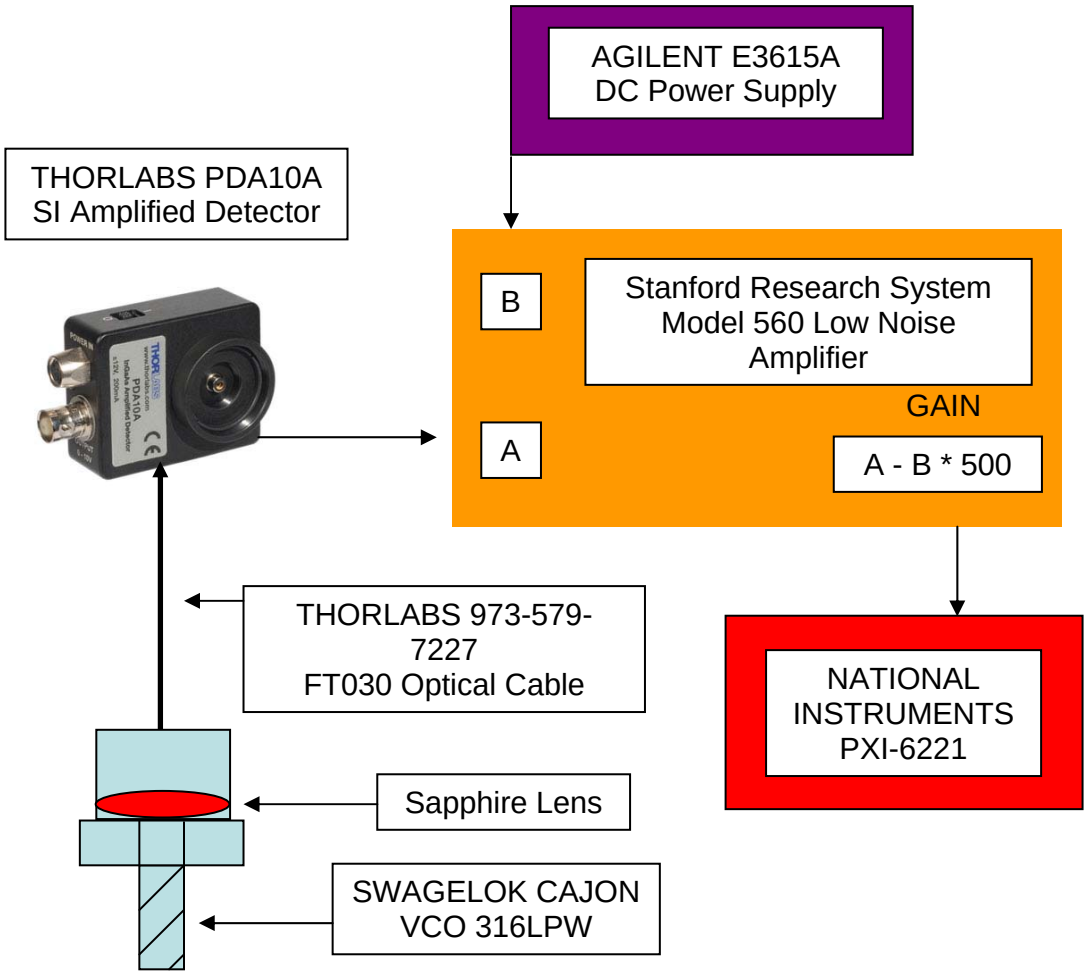

Figure 22. Optical Setup Diagram

The optical sensor was able to successfully detect the corona discharge and subsequent combustion process. Figure 23 depicts the optical sensor data along with pressure transducer information confirming the DDT process. The 0.35 microsecond TPI discharge command was the reference point for the timing process, with the optical sensor detecting the electrode corona discharge roughly 0.35 milliseconds after the end of the discharge command. Ignition delays were measured from the corona discharge emission to the initial peak of combustion. It can be seen that combustion actually started before peak, but even the latter time represented a marked improvement from previous attempts to categorize combustion using pressure measurements.

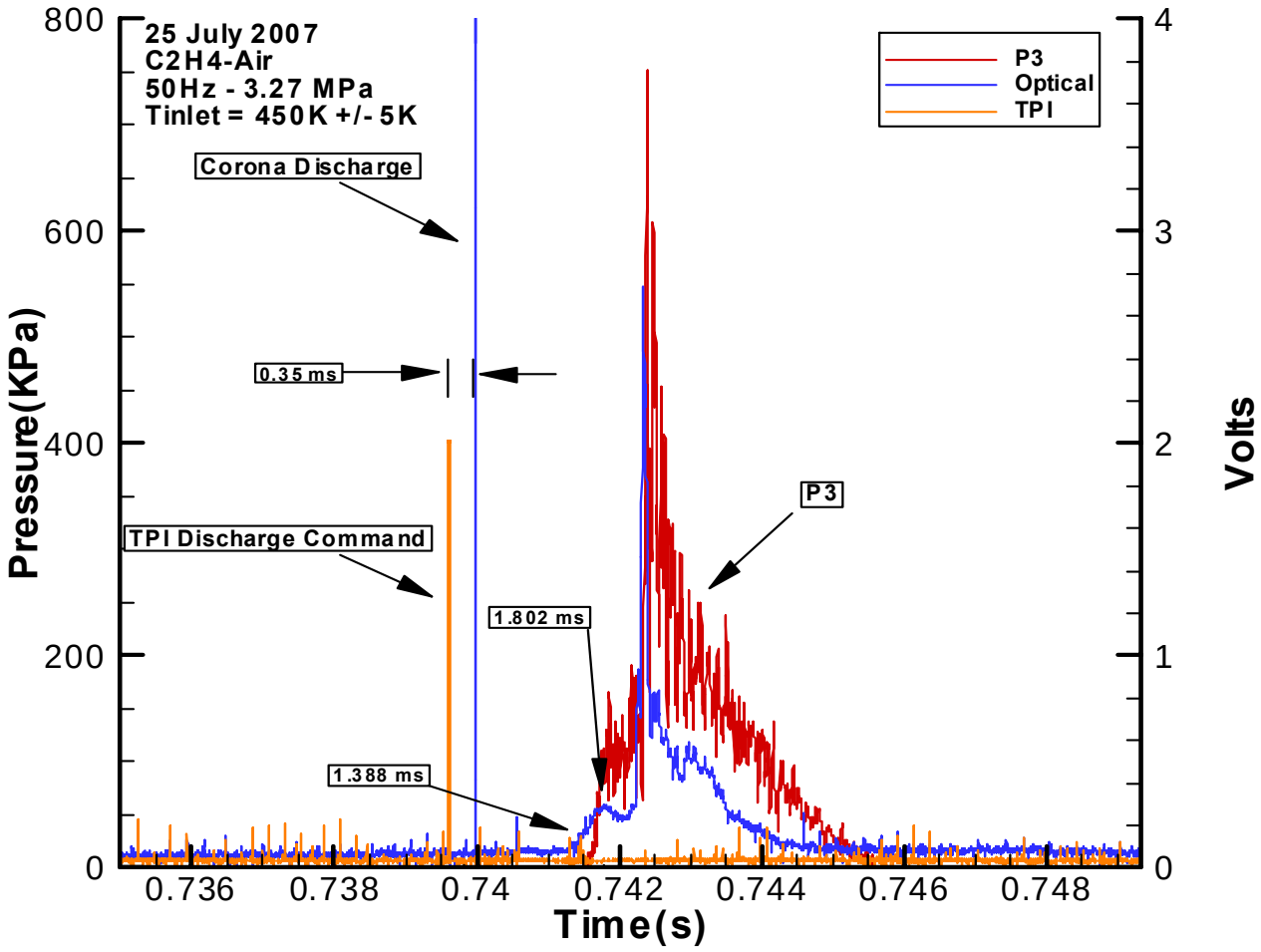

Figure 23. Ignition Command, Optical, and Pressure Transducer Characterization

C. VITIATOR

A vitiator was used to heat air in order to simulate combustor inlet conditions during supersonic cruise velocities. For example, an air flow at 250 kPa and 490K corresponded to inlet flow conditions of Mach 2.5 at a 13,000 m altitude. The vitiator burned a hydrogen/air mixture to heat the air and then supplemental oxygen was added downstream to correct the mass percentage of oxygen in the inlet air. The vitiator was started with a Hydrogen/Air torch, which was sparked by a high voltage transformer and spark plug. Figure 24 depicts the vitiator setup.

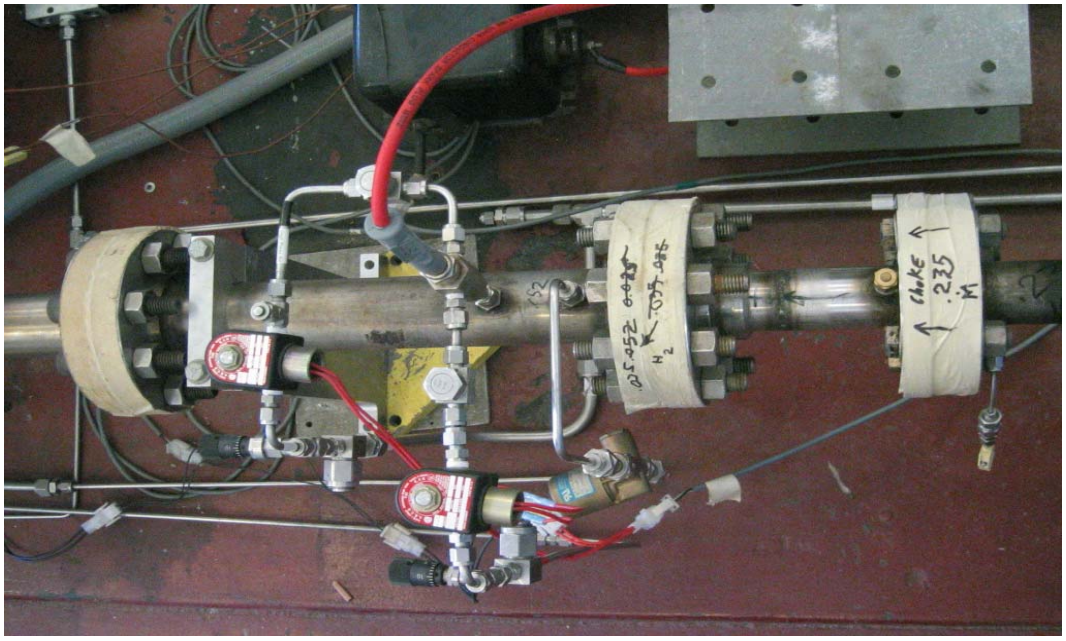

Figure 24. Hydrogen/Air Vitiator

D. FACILITY AND PDE CONTROL

The test cell and PDE were primarily controlled by a PC running LabView RT 8.0 by National Instruments (NI), which was linked to a NI PXI-1000B controller in the test cell. A Berkeley Nucleonics (BNC) 550 Pulse Generator and BNC 555 Pulse/Delay Generator sent the fuel valve and ignition command signals to solid state relays inside the test cell. The TESCOM ER3000 regulator controller software was operated on a separate computer and controlled the regulators for hydrogen, oxygen and ethylene. JP-10 head pressure and the oil pump compressor for the liquid fuel injectors were manually set in the test cell. Figure 25 details the LabView Test Cell Controller.

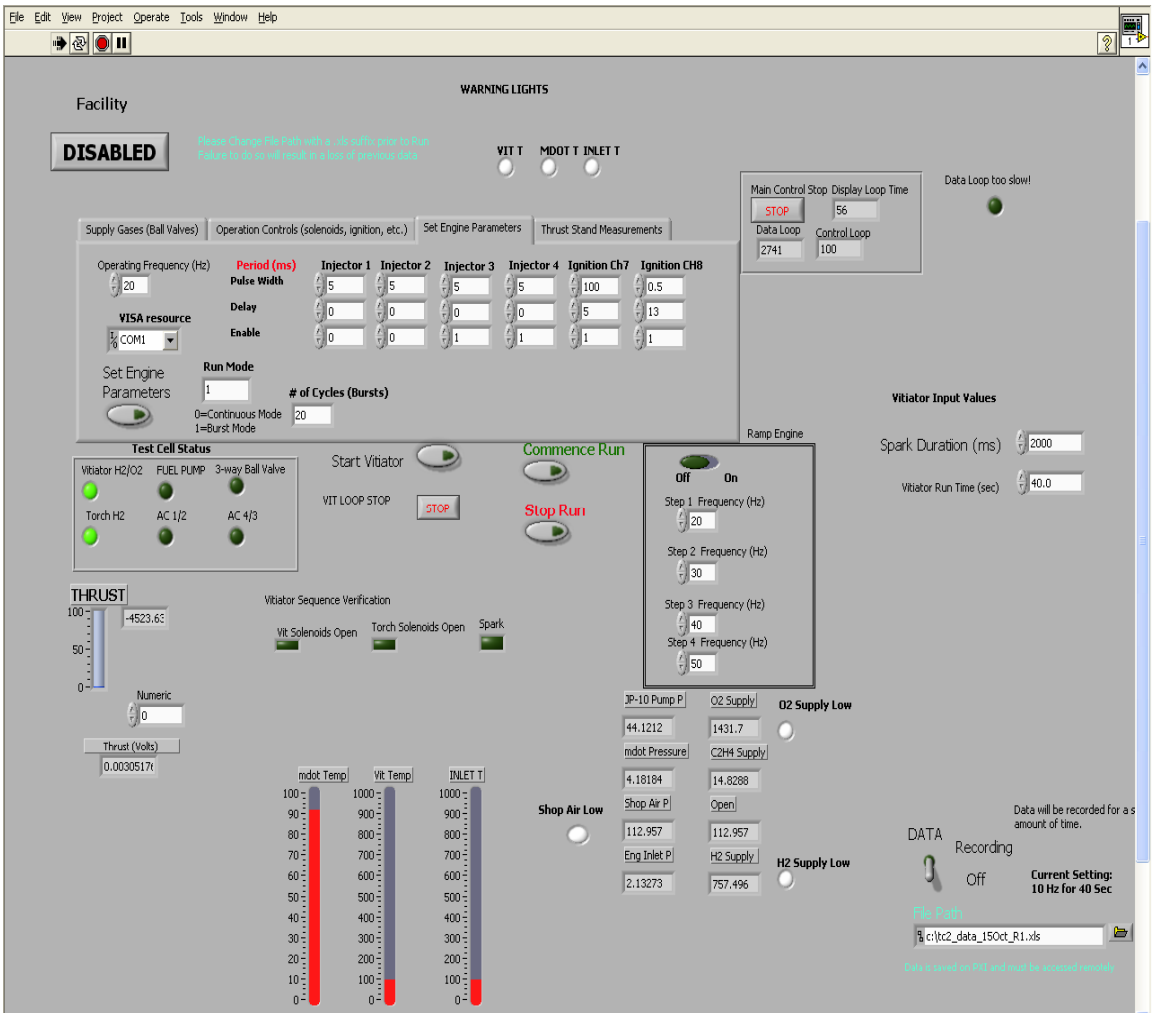

Figure 25. Propulsion Lab Test Cell #2 Graphics-User Interface

A manual safety button was mounted above the PC which controls the test cell and allows for the instantaneous capacity to shutdown the test cell in an emergency situation. All ball valves and solenoid valves would close immediately if the software was disabled or the emergency safety button was depressed.

E. DATA ACQUISITION

The data acquisition of the optical sensor output and high-frequency transducer signals was performed by another computer running a NI LabView program which sampled the four channels simultaneously at 500 kHz for one second. Two pressure relays, one optical relay and one TPI command signal were gathered and analyzed with

TecPlot. Test Cell transducer signals for pressures and temperatures were routed through a PXI-6031E controller inside the PXI-1000B. Figure 26 depicts the LabView data acquisition controller.

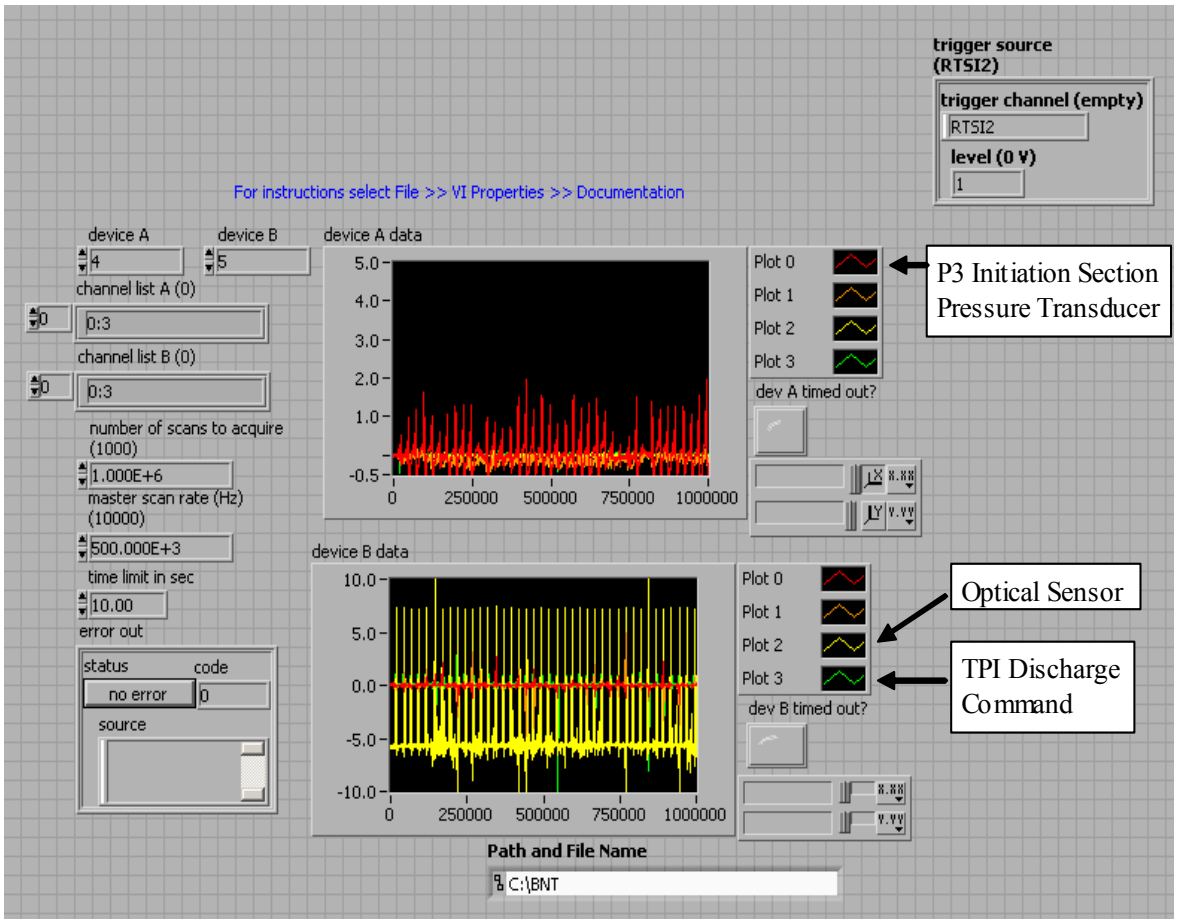

Figure 26. Optical, TPI, and Pressure Transducer Data Collection Interface

THIS PAGE INTENTIONALLY LEFT BLANK

V. RESULTS

A. ETHYLENE/AIR

Ethylene (C_2H_4) was the fuel used to evaluate and characterize the new Macor sleeve, electrode and optical system. Detailed ignition delay measurements and fuel pressure readings were acquired for air mass flow rates of 0.3125 and 0.35 kg/s. The relationship between fuel pressure and ignition delay was also constructed for 0.4 kg/s mass flows. Ignition delays of each 1 second test duration were measured between the 30% to 70% mark at 10% intervals. The average of five time measurements, the maximum and minimum times comprise the three ignition delay data points for each fuel pressure and equivalence ratio. The equivalent ratio, or Φ, describes the composition of a fuel/air mixture. Φ is described as the ratio of the actual fuel-to-oxidizer reactants divided by the ratio of fuel-to-oxidizer reactants in a stoichiometric ratio. An equivalence ratio of 1 is the stoichiometric ratio for complete combustion of a fuel/air mixture. A ratio greater than one implies a fuel-rich mixture and a ratio below one equates to a fuel-lean situation. Equation 2 shows the fuel to oxidizer ratio and equation 3 depicts Φ.

$$f = \frac{\dot{m}_{fuel}}{\dot{m}_{air}} \qquad [2]$$

$$\phi = \frac{f}{f_{stoichiometric}} \qquad [3]$$

The reported stoichiometric ratios were based off of 90% of the mass fraction peaks from Danaher for the single orifice and multiple orifice/screen configurations [12]. Initial ethylene/air testing was done with the single orifice configuration, and the porous ignition shield testing was conducted with the multiple orifice and screen adaptation. Figure 27

depicts the temporal/spatial mass fraction and equivalence ratio for various configurations with 10 ms duration ethylene fuel injections with an air mass flow rate of 0.35 kg/s [12].

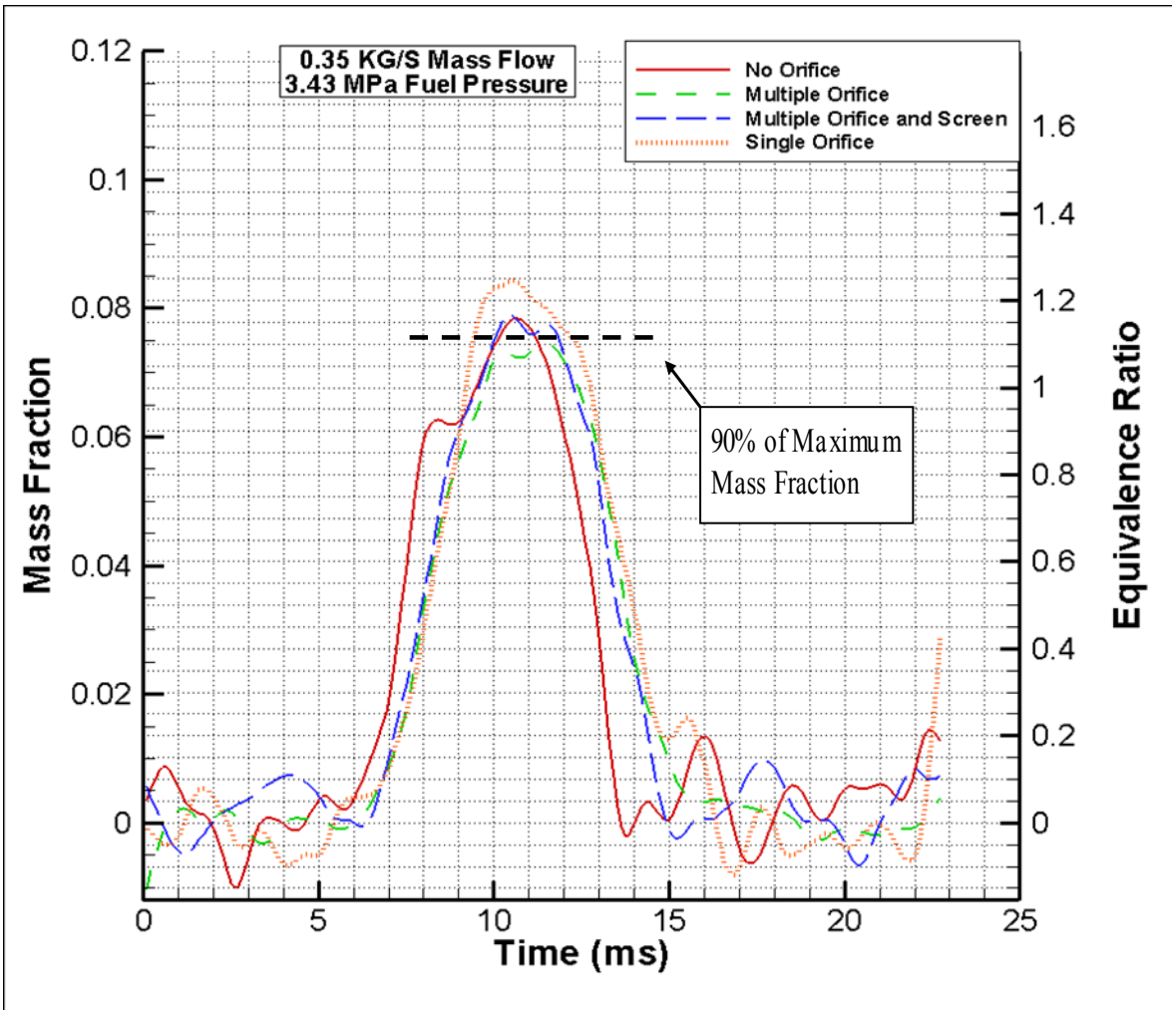

Figure 27. 90% Equivalence Ratio for $\dot{m}_{air}$ = 0.35 kg/s for Single Orifice

Figures 28-32 depict the ignition delay vs. fuel pressure and ignition delay vs. equivalence ratio (Φ).

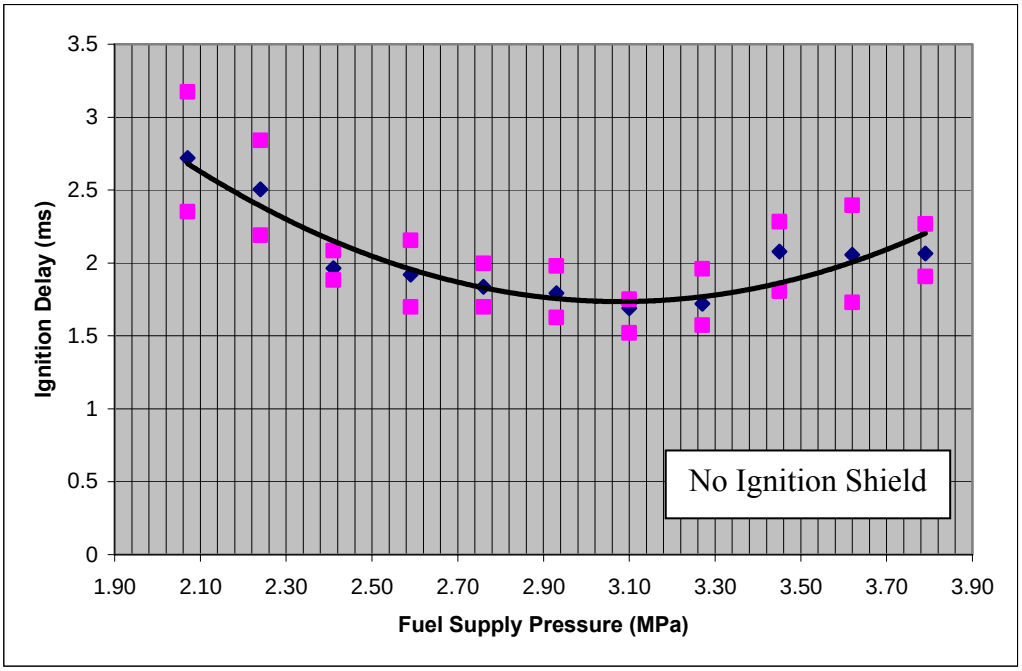

Figure 28. Ignition Delay vs. Fuel Pressure for C_2H_4/air for $\dot{m}_{air}$ = 0.3125 kg/s

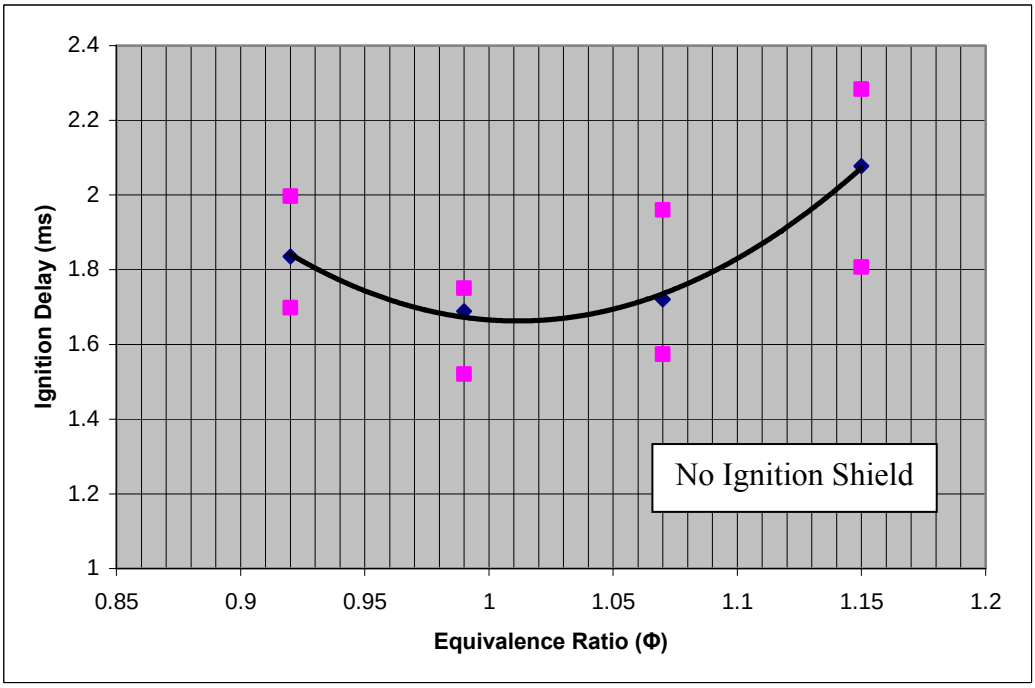

Figure 29. Ignition Delay vs. Equivalence Raito for C_2H_4/air for $\dot{m}_{air}$ = 0.3125 kg/s

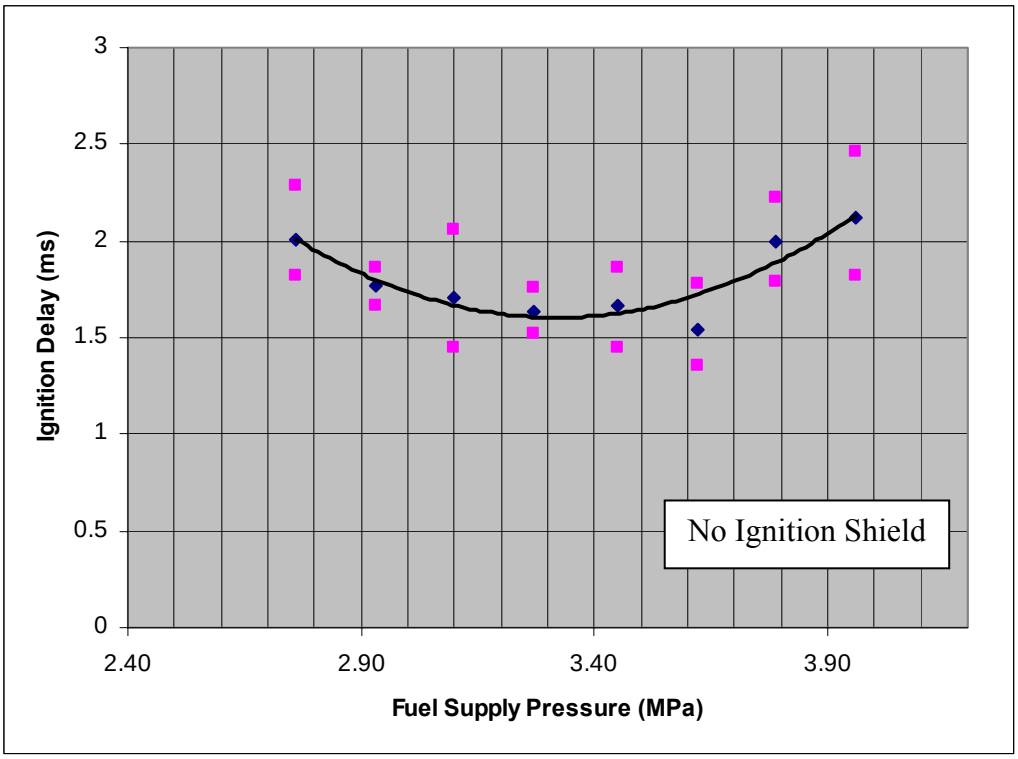

Figure 30. Ignition Delay vs. Fuel Pressure for C_2H_4/air for $\dot{m}_{air}$ = 0.35 kg/s

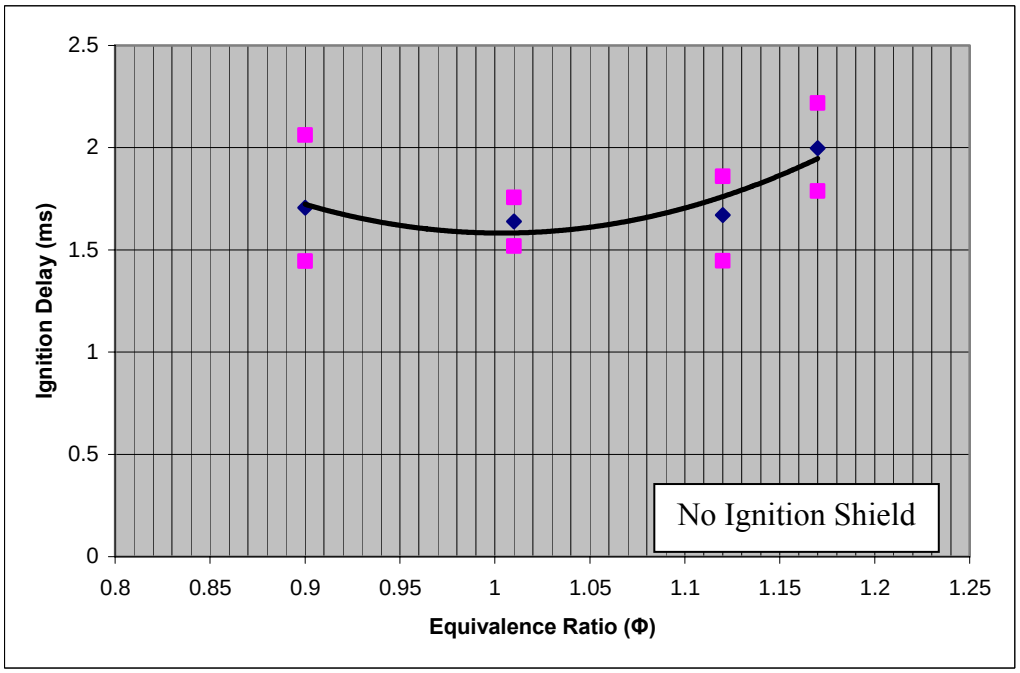

Figure 31. Ignition Delay vs. Equivalence Ratio for C_2H_4/air for $\dot{m}_{air}$ = 0.35 kg/s

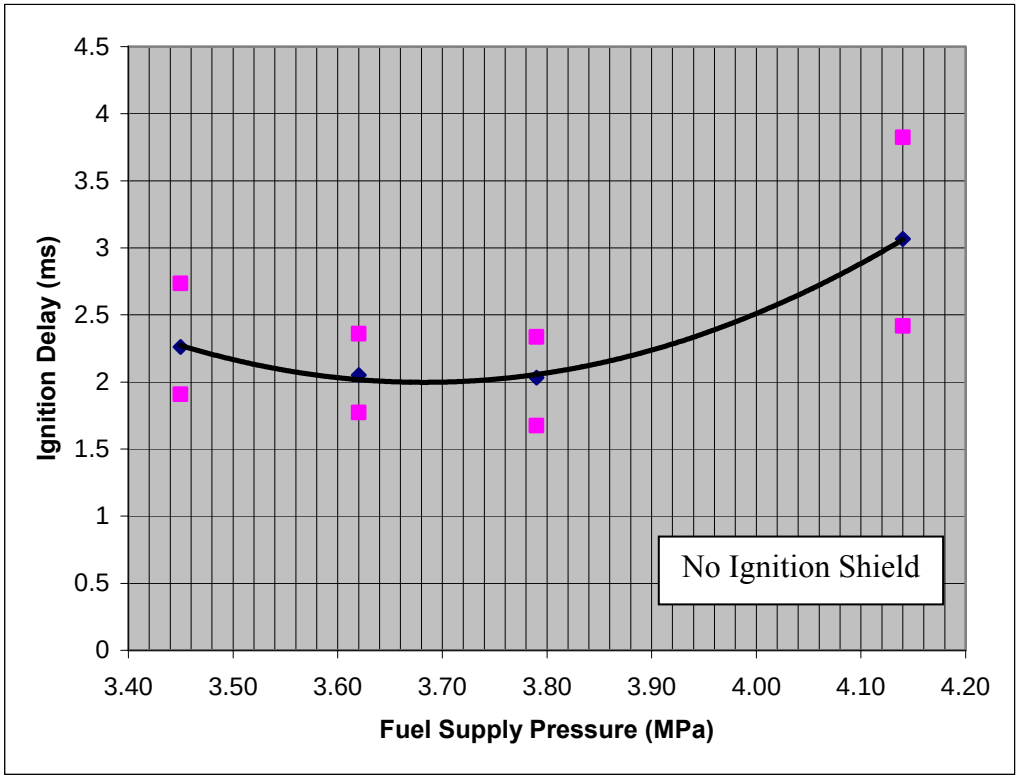

Figure 32. Ignition Delay vs. Fuel Pressure for C_2H_4/air for $\dot{m}_{air}$ = 0.4 kg/s

While the 0.3125 and 0.35 kg/s airflow rate conditions proved to be readily ignitable, the 0.4 kg/s airflow was more difficult to initiate. The 0.4 kg/s success rate noticeably diminished to roughly 20% of the 30 Hz attempts while the ignition delay times expectantly rose.

B. JP-10/AIR

The JP-10 fuel injectors produced an even sharper fuel distribution curve than the ethylene injectors, and Figure 33 depicts the narrow window of opportunity to ignite the JP-10/air mixture [12]. The hydraulically driven injectors can inject up to 130 mm^3 of fuel per injector, and by delaying a pair of injectors the fuel profile can be extended. Placing the injectors out of phase noticeably increased the temporal width of a combustible mixture.

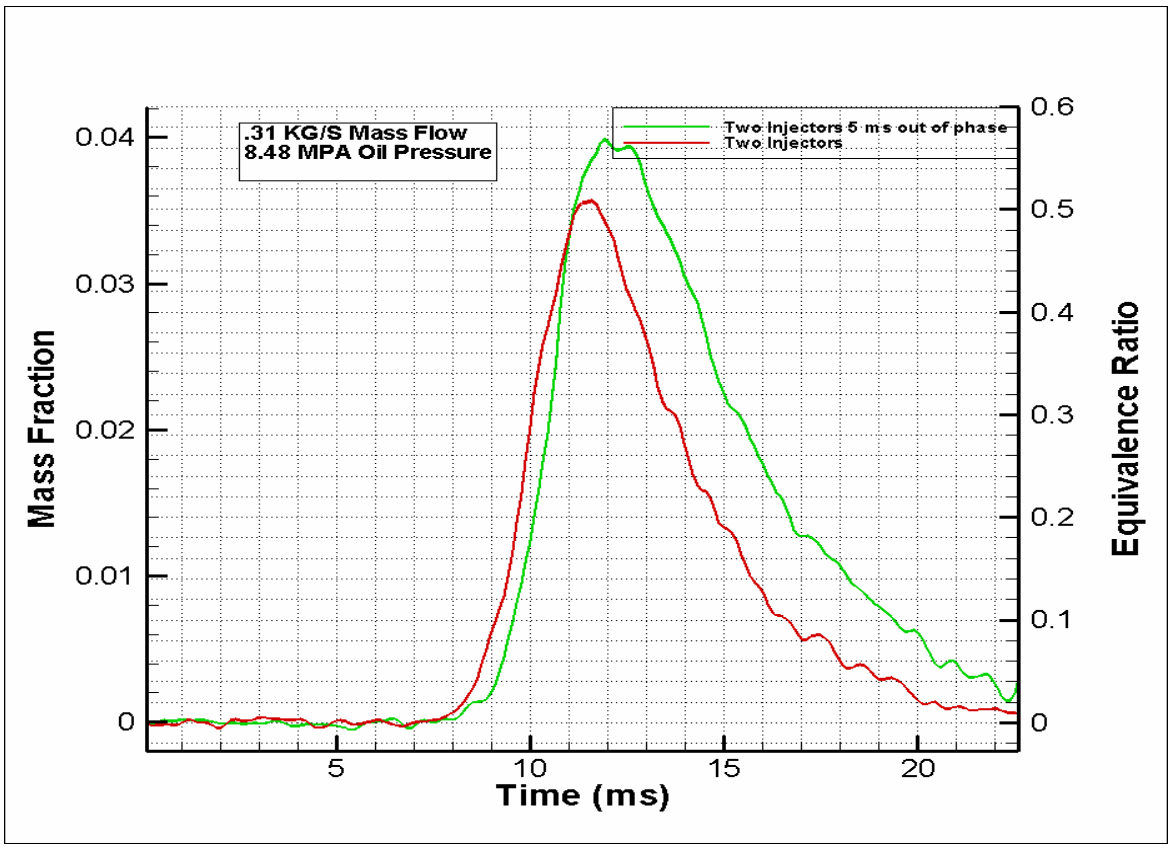

Figure 33. JP10 Fuel Profiles for Two Injectors [12]

The JP-10/air mixture was nearly impossible to ignite at mass flow rates above 0.12 kg/s. A wide range of TPI discharge times were attempted to compensate for the narrow combustion window for JP-10. The sporadic ignitions collected were during the transient period of time after the vitiator had turned off but before total airflow cutoff. The extended ignition delay time meant that the optical sensor was not well positioned to see the entire combustion process. Retonation wave emissions were recorded though and were roughly twice the characteristic times of ethylene/air mixtures; implying that the ignition delay times were twice as long for the JP-10/air mixtures as well. The incomplete evaporation of JP-10 or TPI interaction with the water vapor produced by the vitiator may have inhibited ignition. Further investigation of this phenomenon needs to take place.

C. ETHYLENE/AIR WITH POROUS IGNITION SHIELD

The presence of the porous ignition shield changed the TPI discharge properties due to its reduced distance between the outer wall (cathode) and the electrode (anode), thus reducing the available TPI energy output in order to prevent arcing during one atmosphere pressure conditions. Post experiment inspection showed sporadic arcing, approximately 15% of the cycle, which explained the 80-90% success rate achieved during that testing cycle. Although the pressure and temperature in the initiation chamber was higher during an experimental test, random arcing was still apparently occurring during a test series.

The ignition shield proved successful for initiating combustion when it was initially tested at the 0.3125 kg/s air flow rate conditions. Due to the inherent blocking of the flow field, optical data of the combustion process was difficult to record with the ignition shield in place, but the corona discharge signature was still present. The ignition zone pressure transducer indicated a pressure rise prior to the TPI discharge, which indicated that the ignition shield did not allow a complete purge the previous cycle's products. Figure 34 illustrates this rise prior to the TPI command discharge and subsequent optical reading of the corona discharge of the electrode. Disrupting the TPI discharge midway through a run completely extinguished all combustion activity, revealing that the slight pre-ignition of fuel/air was not sufficient to completely ignite the new fuel/air mixture unless the TPI discharged. The portion of the previous cycle's products which remained helped to create a much shorter ignition delay though, which could be largely responsible for the success of the fuel/air mixture at this mass flow.

Air mass flow rates of 0.4 kg/s and 0.45 kg/s were also successful in producing combustion events, thus further demonstrating the benefits of the shield.

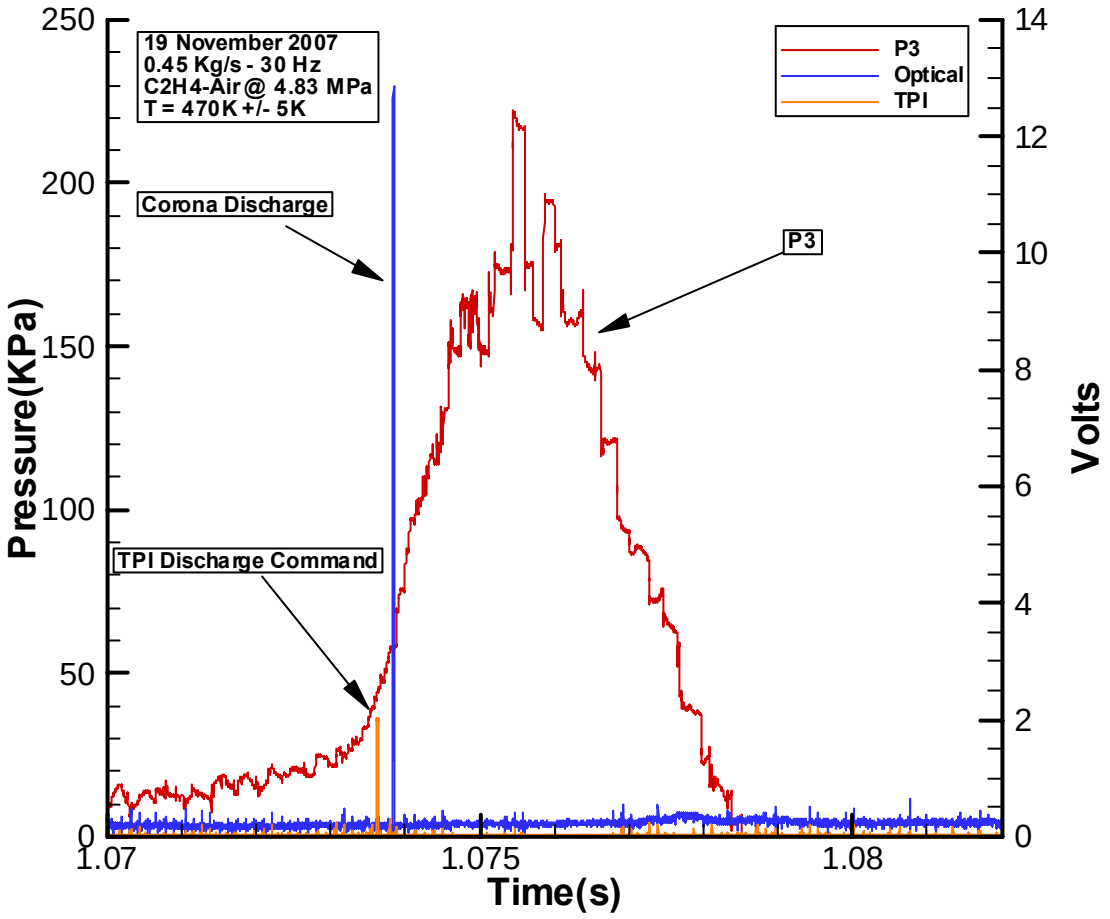

Figure 34. Incomplete Purge for $\dot{m}_{air}$ = 0.45 kg/s with Ignition Shield

D. JP-10/AIR WITH POROUS IGNITION SHIELD

The porous shield also had a substantial improvement for JP-10/air ignition. Air mass air flow rates of 0.15 and 0.2 kg/s were ignitable at 20 Hz. Figures 35 and 36 depict deflagration waves forming near the ignition chamber.

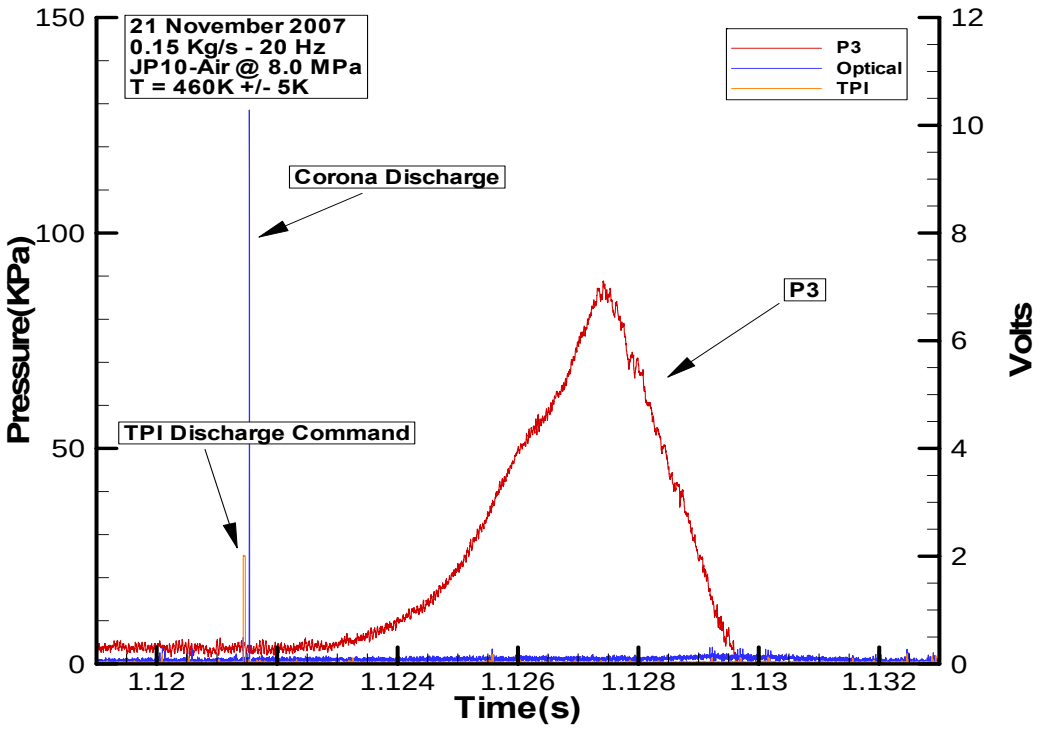

Figure 35. Successful JP-10/air Ignition for $\dot{m}_{air} = 0.15$ kg/s

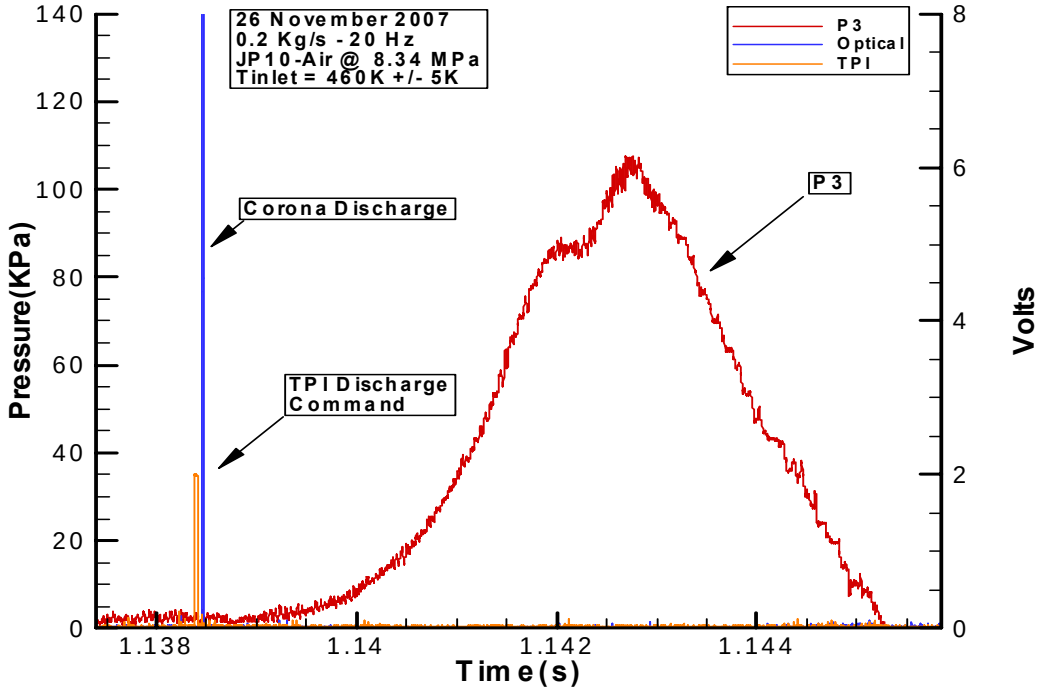

Figure 36. Successful JP-10/air Ignition for $\dot{m}_{air} = 0.2$ kg/s

Interestingly, the PDE ignition delay decreased once the vitiator had cutoff near the end of a test cell run. The improved ignition delay time was coupled with a higher ignition zone transducer pressure rise. The relative humidity of the vitiated air may have led to poor JP-10 evaporation or erratic TPI reactions with the water vapor may have been the cause for poorer performance. This behavior was consistent to runs both with and with out the ignition shield present. The figure below depicts the success with the lack of vitiator water vapor byproduct.

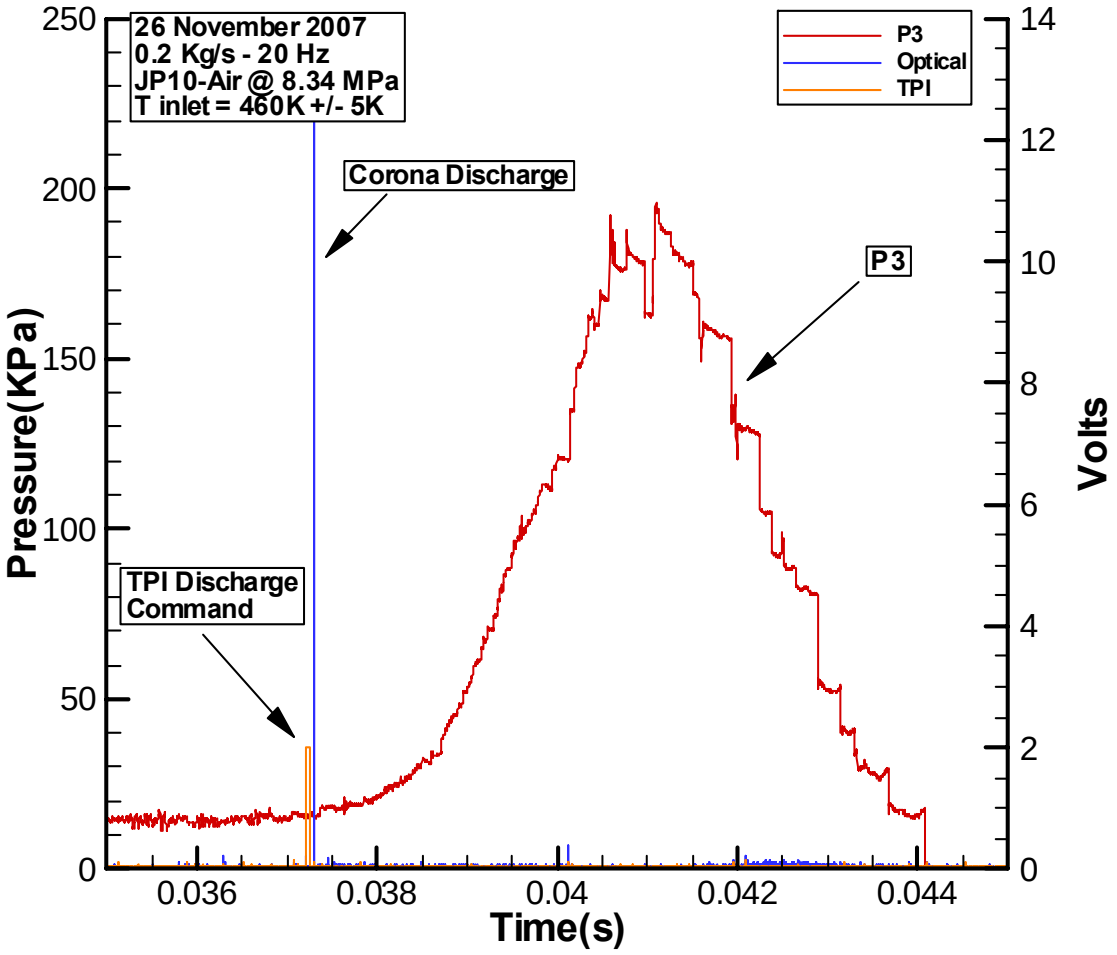

Figure 37. JP-10/air Ignition after Vitiator Cutoff

VI. CONCLUSIONS AND FUTURE WORK

A. CONCLUSIONS

The optical emission system successfully mapped the ignition characteristics of ethylene/air and JP-10/air mixtures. The ignition delay knowledge allowed fine-tuning of the fuel injection and ignition timing processes, and allowed for near-optimized combustion cycle times during the remaining testing periods.

A porous shield was installed around the TPI electrode and produced local low velocity fuel/air mixtures sufficiently for successful ignition and combustion in otherwise un-ignitable conditions. Success was confirmed with a direct comparison of ethylene/air at an air mass flow rate of 0.45 kg/s mass flow, corresponding to a local characteristic velocity of approximately 100 m/s.

Finally, JP-10/air ignition was achieved at air mass flow rates and velocities nearly twice previously reported values. The TPI discharge timing had to be adjusted slightly to compensate for JP-10/air mixtures, and ultimately produced cycles with an approximate 90% success rate. Post-vitiator ignition attempts were extremely successful and showed the true potential of a JP-10 fueled PDE, but revealed the possible detrimental side effect of having substantial water vapor in the vitiated air. The exact mechanisms behind the behavior need to be further explored.

B. FUTURE WORK

Future work should focus on optimizing the ignition shield porosity. Increasing the portion of flow through the ignition region would allow for a more complete purge after each cycle and would likely prevent the pre-ignition condition. Higher mass airflows could also be investigated with the existing porous ignition shield or with some other porosity variant. JP-10/air testing continues to remain critical in order to explore its practical application for PDEs.

Programmable JP-10 fuel injectors would enable more tailorable conditions and higher detonation frequencies. The current injectors do not provide a wide range of

operation. The fuel duration and timing of the injections allow limited flexibility, and adjustable injectors will allow for a wide range of conditions to be delivered to the combustor.

Lastly, reconfiguring the vitiator with a new fuel source will reduce the water vapor, and should increase the ignition success rate during the vitiated portion of a test run.

APPENDIX A: NPS ROCKET LAB TEST CELL #2 SOP

Test Cell #2
Standard Operating Procedures (S.O.P.)
Engine Start UP
(Last modification date 19 June 2007)

Prior to starting preparations

1. Notify all lab personnel of live test cell.
2. Turn ON control console
3. Turn ON warning lights
4. Notify the Golf Course (x2167, ext#1) (Only required if Hot Fire Test is conducted)

Preparing Test Cell

1. Push the Emergency Stop IN (secured)
2. Turn ON BNC Cabinet Power Strip.
3. On Control Computer, open LABVIEW and ensure that the execution target contains the PXI address. Open control panel and run the program.
    a. RT Target address: 172.20.120.118
    b. Control Program Path
        i. Open
        ii. Test Cell #2 Manual Control v20 (runs v19b)
        iii. Enter Run Path Name
            1. If this is not completed prior to running you will lose the data file that was created with the default name.
4. Turn ON 24 VDC in the control room cabinet
5. OPEN Main Air (HP Air Tank Valve) and High Pressure Air
    a. Blue hand valve should be opened slowly as not to shock the lines
    b. Node 4 air valve in test cell #1 open
6. OPEN H_2 & O_2 six packs
7. Enter Test Cell #2 and OPEN all the supply gas bottles that are going to be used
8. OPEN both JP-10 valves
9. Ensure that PXI Controllers, Kistlers, and Power strip in the black cabinet are ON.
10. Turn ON 24 VDC power supply for Test Cell #2 TESCOM Control Power.
11. OPEN Shop Air, Isolation Valve (High Pressure Air) and Main Air
12. If JP-10
    a. CLOSE 440 VAC knife switch for Oil Pump (ON)
13. TURN ON Cooling Water (If required)
14. TURN ON TPI (do not exceed 85 on heater control knob) – 30-60-85 (1 min intervals)
15. CONNECT Vitiator Spark Plug.
16. If required, set up any visual data recording equipment.
17. Evacuate all non-essential personnel to the control room

18. Check Shop Air Compressor in heater room– approx 120 psi min
19. RUN the control
20. Close Blast Door
21. Lock Gate

Running the Engine

1. Set Main Air, Secondary/Purge Air, and all other gases pressures (ER3000) ON RPL00
    a. Set Main Air and Purge Air (ER3000)
        i. 01 Main Air
        ii. 04 Secondary Air – Set to 220
    b. Supply Gases in Test Cell #2 TESCOM Node Address
        i. 20 Vit H_20
        ii. 21 Vit O_2
        iii. 22 C_2H_4
2. **DISCONNECT CH 7 & 8**
3. Set All Engine Control Parameters (on BNC Pulse Generator)
    a. Send Engine Parameters to BNC
4. **RECONNECT CH 7 & 8**
5. Twist Emergency Stop Button clockwise (TEST CELL IS NOW LIVE)
6. ENABLE the Test Cell on the VI.
7. OPEN Vit, Torch, and C_2H_4 Ball Valves.
8. Verify Golf Course is clear
9. SOUND the Siren
10. START recording on VCRs
11. Fuel Pump On (If using JP-10)
12. TURN ON Data Recording Switch
13. Manually engage Main Air flow
14. START Vitiator

**********WARNING**********

The next step will result in the commencement of a run profile and ignition.

* Note: The 3-Way Ball Valve has a control in the Vitiator sequence. If the Vitiator is used then the 3-Way Ball will not divert through the engine until 375º F and will dump overboard at the end of the run at 175º F.

15. COMMENCE RUN
    a. High Speed DAQ will be triggered and the engine profile will commence
16. STOP RUN.
    a. Pulse generation will be stopped.
17. TURN OFF Data Recording Switch
18. Wait for main air to divert
19. STOP Main Air Flow
20. Ensure all Ball Valves are closed
21. Fuel pump OFF (If using JP-10)

22. DISABLE the Test Cell on the VI.
23. Push Emergency Stop Button IN

Test Cell #2
Standard Operating Procedures (S.O.P)
Engine Shut DOWN
(Last modification date 19 June 2007)

1. SET all supply gases to ZERO, Nodes 1, 4, 20, 21 & 22
2. ClOSE all gas supply valves using LabView
3. STOP control code.
4. Push Emergency Stop Button IN
5. Turn OFF Power Strip in BNC Timing Cabinet
6. If Gas Turbine Igniter (Test Cell #1) used DISABLE BEFORE turning off 24 VDC
7. TURN OFF 24 VDC power supply (check with other test cells first)
8. CLOSE Jamesbury Valve (check with other test cells first)
9. REMOVE Vitiator Spark Plug head
10. SECURE TESCOM 24VDC power. (check with other test cells first)
11. CLOSE Shop Air, High Pressure Air, and Main Air
12. If using JP-10
    a. OPEN 440 VAC Knife switch (OFF)
13. TURN OFF Cooling Water
14. CLOSE Supply gases
15. CLOSE JP-10 supply valves
16. TURN OFF TPI
17. CLOSE H_2 & O_2 six packs
18. VENT H_2 & O_2 lines
19. STOW Cameras and other equipment used in testing.
20. CLOSE Test Cell #2.
21. TURN OFF Warning Lights.

THIS PAGE INTENTIONALLY LEFT BLANK

LIST OF REFERENCES

[1] Fleeman, E.L., *Tactical Missile Design*, AIAA, 2001.

[2] Hutcheson, P.D., "Design, Modeling and Performance of a Split Path JP-10/air Pulse Detonation Engine," Master's Thesis, Naval Postgraduate School, Monterey, California, December 2006.

[3] Mattingly, J. D., *Elements of Propulsion: Gas Turbines and Rockets*, AIAA, 2006.

[4] Brophy, C., Sinibaldi, J.O., Wang, F., Jiang, C., and Gundersen, M.A., "Transient Plasma Ignition of a Hydrocarbon-Air Initiator for Pulse Detonation Engines," *Application of Detonation to Propulsion*, Torus Press, 2004.

[5] Wang, F., Kuthi, A., and Gundersen, M.A., "Technology for Transient Plasma Ignition," AIAA Paper 2005-0951, *43rd AIAA Aerospace Sciences Meeting and Exhibit*, Reno, Nevada, 10-13 January 2005.

[6] Hall, P.D., "Design of a Coaxial Split Flow Pulse Detonation Engine," Master's Thesis, Naval Postgraduate School, Monterey, California, June 2006.

[7] Hoffman, H., "Reaction-Propulsion Produced by Intermittent Detonative Combustion." German Research Institute for Gliding, Report ATI-52365, August 1940.

[8] Kuo, K.K., *Principles of Combustion,* Second Edition, John Wiley and Sons, 2005.

[9] Glassman, I., *Combustion*, Second Edition, Academic Press, Inc., 1987

[10] Erpenbeck, J. J., "Stability of Idealized One Reaction Detonations," *Physics of Fluids*, Vol. 7, No. 5, 1964, pp. 684-696.

[11] Ciccarelli, G., Card, J., "Detonation in Mixtures of JP-10 Vapor and Air," AIAA Journal, Vol. 44, No. 2, February 2006.

[12] Danaher, T.J., "Characterization of Ethylene/JP-10 fuel injection profiles for a valveless Pulse Detonation Engine," Master's Thesis, Naval Postgraduate School, Monterey, California, December 2007.

[13] Kelly, J., "After Combustion: Detonation," Popular Science, August 2003.

THIS PAGE INTENTIONALLY LEFT BLANK

INITIAL DISTRIBUTION LIST

1. Defense Technical Information Center
   Ft. Belvoir, Virginia

2. Dudley Knox Library
   Naval Postgraduate School
   Monterey, California